



TALLINN UNIVERSITY OF TECHNOLOGY

SCHOOL OF ENGINEERING

Department of Electrical Power Engineering and Mechatronics

CREATING A MATHEMATICAL MODEL OF TANDEM EDF MOTOR FOR VTOL APPLICATIONS

TANDEM EDF MOOTORI MATEMAATILISE MUDELI LOOMINE VTOLI RAKENDUSTE JAOKS

MASTER THESIS

Student: Stiven Kossorotov

Student code: 212071MAHM

Supervisor: Kristjan Pütsep, Lecturer

Tallinn, 2023

(On the reverse side of title page)

AUTHOR'S DECLARATION

Hereby I declare that I have written this thesis independently.

No academic degree has been applied for based on this material. All works, major viewpoints and data of the other authors used in this thesis have been referenced.

"16" May 2023

Author: Stiven Kossorotov

/signature /

Thesis is in accordance with terms and requirements

"16" May 2023

Supervisor: Kristjan Pütsep

/signature/

Accepted for defense

".....".....2023 .

Chairman of theses defense commission:

/name and signature/

Non-exclusive License for Publication and Reproduction of Graduation Thesis¹

I, Stiven Kossorotov (date of birth: 11.06.1995)

Hereby

1. grant Tallinn University of Technology (TalTech) a non-exclusive license for my thesis

"Creating a Mathematical Model of Tandem EDF Motor for VTOL Applications",

supervised by

Kristjan Pütsep – Lecturer, Tallinn University of Technology

- 1.1. reproduced for the purposes of preservation and electronic publication, incl. to be entered in the digital collection of TalTech library until expiry of the term of copyright.
 - 1.2. published via the web of TalTech, incl. to be entered in the digital collection of TalTech library until expiry of the term of copyright.
 - 1.3. I am aware that the author also retains the rights specified in clause 1 of this license.
2. I confirm that granting the non-exclusive license does not infringe third persons' intellectual property rights, the rights arising from the Personal Data Protection Act or rights arising from other legislation.

_____ (signature)

16. May 2023 (date)

¹ The non-exclusive license is not valid during the validity of access restriction indicated in the student's application for restriction on access to the graduation thesis that has been signed by the school's dean, except in case of the university's right to reproduce the thesis for preservation purposes only. If a graduation thesis is based on the joint creative activity of two or more persons and the co-author(s) has/have not granted, by the set deadline, the student defending his/her graduation thesis consent to reproduce and publish the graduation thesis in compliance with clauses 1.1 and 1.2 of the non-exclusive license, the non-exclusive license shall not be valid for the period.

ABSTRACT

Author: Stiven Kossorotov

Type of the work: Master Thesis

Title: Creating a mathematical model of tandem EDF motor for VTOL applications

Date: 16.05.2023

67 pages

University: Tallinn University of Technology

School: School of Engineering

Department: Department of Electrical Power Engineering and Mechatronics

Supervisor(s) of the thesis: Lecturer Kristjan Pütsep

Given work was mainly concerned with the creation and verification of the realistic mathematical model of the already existing aircraft, developed by Tõivo Nerep in 2022. Thus, the main purpose of the work can be said to be the finalization of the development cycle of an aircraft. The aircraft in question is a tail-sitter VTOL (vertical take-off and landing), which was powered with two electrical ducted fans rotating in different direction. The model, similar to the Tõivo's work, comprises only the hovering phase of its flight.

The model was developed using MATLAB Simulink software while different systems of the aircraft (flying code, actuators, airframe) and the environment were simulated as a separate logical block within the model, with signals as a mean of the communication between the blocks. System of independent PID controllers was used to control yaw, pitch, and roll angles, as well as an altitude of the aircraft. In addition, the movement of the roll and pitch control surfaces together with the main electrical engine fan's rotations were visualized in the separate block using Simscape Multibody environment.

As it was quickly discovered during the work, there was a lack of accurate physical parameters of the engines to complete the model: thrust, torque and speed as a function of power supplied to the motor. In order to obtain those parameters a series of measurements has been performed on the real electrical engines using a RCbenchmark test stand. During this practical work, a procedure for electrical motor measurements was developed. This can be used to acquire comparable results from diverse types of electrical motors.

Experimental results were analyzed, cleaned, and successfully implemented in the model. Main outcomes of the work can be seen to be a consistent mathematical description of the VTOL aircraft, as well as a framework for experimental measurements of the electrical motors.

Keywords: VTOL, tandem EDF, UAV, mathematical model, control algorithm, thrust measurement, torque measurement

LÕPUTÖÖ LÜHIKOKKUVÕTE

Autor: Stiven Kossorotov

Lõputöö liik: Magistritöö

Töö pealkiri: Tandem EDF mootori matemaatilise mudeli loomine VTOLi rakenduste jaoks

Kuupäev: 16.05.2023

67 lk

Ülikool: Tallinna Tehnikaülikool

Teaduskond: Inseneriteaduskond

Instituut: Elektroenergeetika ja mehhatroonika instituut

Töö juhendaja(d): lektor Kristjan Pütsep

Antud töö on seotud Tõivo Nerep 2022. aastal välja töödeldud drooni realistliku matemaatilise mudeli loomise ja verifitseerimisega. Seega saab selle töö põhieesmärgiks pidada lendava masina arendustsükli lõpuleviimist. Kõnealune droon on saba pealt õhku tõusev VTOL (vertikaalne õhkutõusmine ja maandumine), mille toiteallikaks on kaks erinevas suunas pöörlevat kanalit ventilaatoriga elektrimootorit. Välja töödeldud mudel, sarnaselt aluseks võetud Tõivo tööle, põhineb lennu hõljumisfaasi simulatsioonile.

Mudeli ülesehitamiseks on valitud MATLAB Simulink keskkond, kus lennuki erinevaid süsteemi (Lennukood, Täiturmehhanismid, Lennukikere) ja Keskkonda simuleeriti eraldiseisvate loogiliste plokkidena, mis on teineteisega signaalidega ühendatud. Sõltumatute PID-kontrollerite süsteemi kasutati lengerdus-, tandaaž- ja rullnurkade ning lennuki kõrguse juhtimiseks. Simscape Multibody keskkond on võetud eraldiseisvas plokkis tandaaž- ja rull-juhtpindade liikumise koos elektrimootorite ventilaatorite pöörlemise visualiseerimiseks.

Töö käigus on kiiresti jõudnud järelduseni, et piisavalt täpse mudeli realiseerimiseks on puudu järgnevatest mootori füüsikalistest parameetritest: tõukejõud, pöördemoment ja kiirus sõltuvalt mootorile antud võimsusest. Nende parameetrite saamiseks viidi reaalse elektrimootoriga läbi mõõtmisi, kasutades RCbenchmark-i katsestendi. Selle praktilise töö käigus on töötatud välja lisaks ka elektrimootorite mõõtmise protseduur, mida saab kasutada võrreldavate tulemuste saamiseks teisi elektrimootori testides.

Katsetulemusi analüüsiti, puhastati ja rakendati mudelis edukalt. Töö peamiseks tulemusteks on VTOL-lennukite realistlik matemaatiline kirjeldus antud mudeli abil ning elektrimootorite füüsiliste parameetrite mõõtmisteks välja töötatud protseduur.

Märksõnad: VTOL, tandem EDF, mehitamata õhusõiduk, matemaatiline mudel, juhtimisalgoritm, tõukejõu mõõtmine, pöördemomendi mõõtmine

THESIS TASK

Thesis title in English: **Creating a mathematical model of tandem EDF motor for VTOL applications**

Thesis title in Estonian: **Tandem EDF mootori matemaatilise mudeli loomine VTOLi rakenduste jaoks**
Stiven Kossorotov, 212071MAHM

Student:

Program: **Mechatronics**

Type of the work: **Master Thesis**

Supervisor of the thesis: **Kristjan Pütsep**

Co-supervisor of the thesis: -
(company, position and contact)

Validity period of the thesis task: **Validity period is given by supervisor**
2022/2023 2023/2024 Spring

Submission deadline of the thesis: **18.05.2023**

Supervisor (signature)

Student (signature)

Head of program (signature)

Co-supervisor (signature)

1. Reasons for choosing the topic

Availability of cheap and powerful electric engines resulted in the blossoming of remotely controlled drones. Newest control algorithms helped to bring us even further – UAVs are in wide use. Thus, creating of mathematical model for a control algorithm of one of promising VTOL engines – tandem EDF – could enhance such development even further.

2. Thesis objective

The aim of this thesis is to create and verify a mathematical model for previously developed control algorithm for the tandem EDF motor for VTOL applications.

3. List of sub-questions

- Familiarize myself with the requirements for a mathematical model and tools, used for development of such models in the industry

- Create a model for a control algorithm of a tandem EDF motor
- Enhance the model using measurements from the real EDF engine
- Adjust and reiterate, if needed, describe the results

4. Basic data:

Tõivo Nerep`s Master Thesis will deal as a main source of information for this thesis work. In addition to that, some general information about the EDFs, VTOLs and widely used control algorithms for aircrafts would be taken from the academic papers (ESTER, ResearchGate etc.). Information about usage of MATLAB/Simulink environment for creation/verification of mathematical models would be taken from the online resources (articles, educational videos etc.).

5. Research methods

Main part of the work, assumed for the given thesis, should be done in MATLAB/Simulink environment. In addition, lab equipment (power supply unit, PWM signal generator etc.) would be used to conduct the experiment. Different Microsoft programs (Word, Excel, PowerPoint etc.) are planned to be used to analyze and represent the data.

6. Graphical material

Expected are graphs from MATLAB/Simulink and pictures of the experimental environment. In addition, aiding illustrations would be added, when needed (e.g., in Literature Review).

7. Thesis structure

- Preface
- List of abbreviations and symbols
- Introduction
- Main body
 - Literature Review
 - Different designs of VTOL UAVs
 - EDF motor applications in UAVs
 - Control algorithms for EDF motors
 - Mathematical models of VTOL UAVs
 - Model Creation
 - Basics of the Mathematical Model
 - Actuators
 - Airframe
 - Environment

- Flying code
 - Visualization
- Experiments
 - Need for an experiment
 - Equipment and Process
 - Problems and Adjustments
 - Results
 - Experimental conclusions
- Summary
- List of references
- Appendices
- Graphical material

8. References

Main inputs for this work were acquired from:

- T. Nerep, "Construction of VTOL Drone with Tandem EDF Motor and Development of an Algorithm for Automatic Stabilization in Hover Flight," Tallinn University of Technology, Tallinn, 2022.
- G. J. J. Ducard and M. Allenspach, "Review of designs and flight control techniques of hybrid and convertible VTOL UAVs," Aerospace Science and Technology, vol 118, p. 107035, November 2021.
- The MathWorks, Inc. (2023). MATLAB version: 9.13.0 (R2022b). Accessed: May 03, 2023. Available: <https://www.mathworks.com>

9. Thesis consultants

-

10. Work stages and schedule

1. Choosing the topic and familiarizing myself with the details (September - October 2022)
2. Literature research (November - December 2022)
3. Creating of a mathematical model (January - February 2023)
4. Experiments and model adjustment (March - April 2023)
5. Compiling the written part (April - May 2023)
6. Preparation for the defense (May - June 2023)

CONTENTS

ABSTRACT	4
LÕPUTÖÖ LÜHIKOKKUVÕTE	5
THESIS TASK	6
PREFACE	11
LIST OF ABBREVIATIONS AND SYMBOLS	12
LIST OF FIGURES	13
1. INTRODUCTION	15
2. LITERATURE REVIEW	19
2.1 Different designs of VTOL UAVs	19
2.2 EDF motor applications in UAVs	24
2.3 Control algorithms for VTOLs	27
2.4 Mathematical models of VTOL UAVs	33
2.5 Conclusion of the Literature Reviews	35
3. VTOL MODEL CREATION	36
3.1 Basis of the Mathematical Model	36
3.2 Actuators	38
3.3 Airframe	39
3.4 Environment	42
3.5 Flying code	44
3.6 Visualization	47
4. EXPERIMENTS	48
4.1 Equipment and Process	49
4.2 Problems and Adjustments	50
4.3 Results	52
4.4 Experimental conclusions	55
SUMMARY	56

KOKKUVÕTE	58
APPENDICES	66

PREFACE

As people were always looking wistfully into the sky, I was no different. As the modern era brings new challenges and opportunities, mechatronic field of unmanned aircrafts becomes increasingly attractive. Being a person with natural interest towards complex moving mechanisms (this has brought me to engineering in a first place), I wanted to investigate more what constitutes the state-of-the-art in mechatronics in general and in the UAV industry in particular.

From the work on the given thesis, I learned how to plan for big projects and how to come back into the agreed path after sudden setbacks. In addition to expanding my theoretical knowledge in the field of aeronautics, gained in course of the given project, some practical experience in the field of electronics has also been acquired. Namely, I had a chance to practice soldering and could explore the practical side of the capacitor usage.

For my master's thesis I had a pleasure to continue the work of Tõivo Nerep, who I want to thank hereby for his contribution, and make a mathematical model for his recently developed algorithm for tandem EDF control. Existence of such model will enhance the usage of Tõivo Nerep's control algorithm and will help to finish the cycle of development.

Furthermore, I want to express gratitude to my parents Oleg and Larissa, who inspired me to continue my education and provided needed emotional support during last 2 years. I am also very thankful to my old friend Anton Šambalov, an aerospace engineer himself, who sparked my interest in UAVs, as well as my Ericsson colleagues (Yehor Karpichev and Ubaid Fayaz, to name a few), who helped me to align work and study on a daily basis. As last but not the least I want to mention my supervisor, Kristjan Pütsep, who kept me engaged from the 1st semester on and was extremely helpful with his ideas and advice during writing of this thesis.

Keywords: VTOL, tandem EDF, UAV, mathematical model, control algorithm, thrust measurement, torque measurement

LIST OF ABBREVIATIONS AND SYMBOLS

AOA – Angle of Attack

DCM – Direct Cosine Matrix

DoF – Degree of Freedom

EDF – Electric Ducted Fan

ESC – Electronic Speed Controller

Kgf – Kilogram force

LQR – Linear Quadratic Regulator

MRAC – Model Reference Adaptive Control

NACA – National Advisory Committee for Aeronautics

NED – North-East-Down

NN – Neural Network

PC – Personal Computer

PID – Proportional Integral Derivative

PSU – Power Supply Unit

PV – Process Value

PWM – Pulse Width Modulation

RPM – Rotations Per Minute

UAV – Unmanned Air Vehicle

ST – Set Value

VTOL – Vertical Take-off and Landing

WGS – World Geodetic System

LIST OF FIGURES

Figure 1.1 Four forces applied to the airplane during flight [1]	15
Figure 1.2 Function of the tail rotor in the helicopter [2]	16
Figure 1.3 Lockheed XFV-1 VTOL [5].....	17
Figure 2.1 Tail-sitter with a Single Thrust-Vector Propeller [6].....	19
Figure 2.2 Hardware configuration of the Wingtra S100 [11].....	21
Figure 2.3 The Hong Hu quadrotor tail-sitter UAV [15]	21
Figure 2.4 Experimental tiltrotor aircraft with 2 propellers on the wings [16].....	22
Figure 2.5 Accelerating transition of a tiltwing VTOL with 2 pair of wings [21]	23
Figure 2.6 The ducted-fan micro-aerial vehicle with its sub-systems, a – frame, b – propeller and c1/c2 – control vanes [10]	24
Figure 2.7 Model of a dual EDF motor UAV [25].....	25
Figure 2.8 Tandem EDF VTOL in the test bench [17]	27
Figure 2.9 Block diagram of proposed PID Controller [9]	29
Figure 2.10 Mapping technique, used to recalculate the parameters for the robust control law [33]	30
Figure 2.11 Block diagram of the adaptive control architecture [4]	31
Figure 2.12 General structure of a NN [36]	32
Figure 2.13 3D CAD of double propeller Ducted-Fan with the visualized Inertial and Body coordinate frames [29].....	34
Figure 3.1 Block diagram of tandem EDF VTOL mathematical model	37
Figure 3.2 Application of Equation 4.3 for Thrust calculation in MATLAB/Simulink, with left “1” box representing an input (EDF power level), “u ² ” squaring, “0.2332” & “0.30343” multiplication with corresponding numbers (gain) and right “1” an output (thrust power) after addition of both paths (squared and linear).....	39
Figure 3.3 Coordinate frames used in “6DOF (Euler Angles)” block in Simulink [40], with Xe, Ye and Ze being the coordinates in Earth frame and Xb, Yb, Zb, ub, vb and wb coordinates and corresponding speeds in Body frame.....	40

Figure 3.4 Lift curve for NACA 0012 airfoil with C_L as a lift coefficient, alpha as AOA, colorful triangles and squares representing different experimental dataset and a black line being the best fit for all given experiments [42]	41
Figure 3.5 Flying code block.....	45
Figure 3.6 Roll, pitch, and yaw control results	46
Figure 3.7 Altitude control results	46
Figure 3.8 Simulation of the tandem EDF VTOL in a Simscape Multibody environment, with parts imported from Solidworks to be seen on the left side of the screen and the visual representation of the control mechanisms movement in the middle	47
Figure 4.1 Throttle mapping test equipment used in [17].....	48
Figure 4.2 Test-bench that was used to measure thrust and torque of an EDF motor, with PSU standing for Power Supply Unit, PC for Personal Computer, EDF for Electric Ducted Fan and PWM for Pulse-Width Modulation.....	50
Figure 4.3 EDF motor powered through ESC board, with ESC standing for Electronic Speed Control	51
Figure 4.4 EDF motor Optical speed, Torque and Thrust measurements during an expermint.....	53

1.INTRODUCTION

Most of the aircrafts around us belong to the one of the two main types of the aircraft: fixed-wing or rotary-wing. Both types of the aircraft are united by the fact that they are heavier than the air and thus an additional uplift force needs to be created in order to stay take off and stay in the floating state. The general physical principle, which is applied to lift those aircrafts up, is also similar and based on compression of the air by the form of the wing. As the name suggests, however, the form in which this mechanism is deployed differs.

To understand how all aircrafts fly understanding of basic rules of aerodynamic is crucial. Aircrafts can be controlled by balancing four main forces (lift, weight, thrust and drag, see Figure 1.1), applied on the aircraft during the flight. To take off, for example, lift force, generated by the wings, should be greater than the weight of the air vehicle in question.

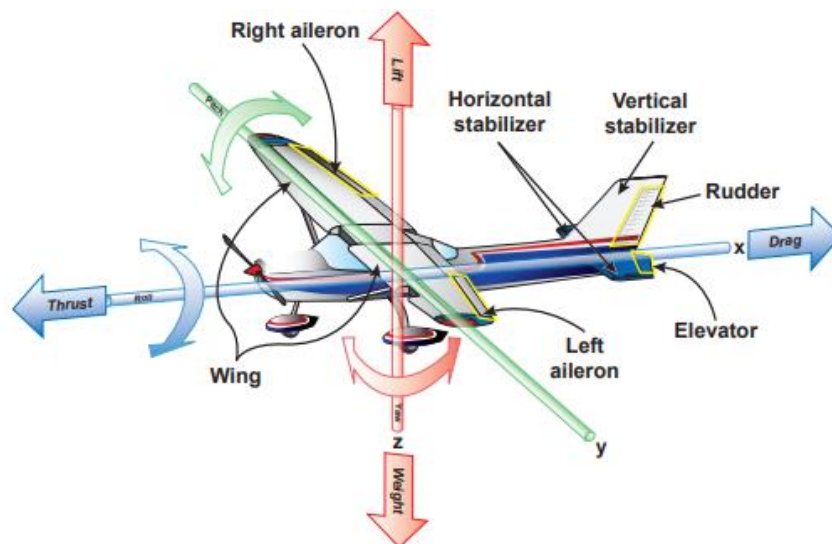


Figure 1.1 Four forces applied to the airplane during flight [1]

Lift is generated by the wing foils and depends on the speed, air density, shape and size of the foil and angle of attack (AOA). As other factors cannot be changed during the flight, aircrafts are usually controlled by varying the speed and AOA on the foils. The higher those two factors are, the greater the lift. [1]

Fixed-wing aircraft generate lift, needed to take-off, by increasing their longitudinal speed with the force of the turbines (thrust). As the aircraft starts from stand-still and needs to overcome drag first, that means that a long runaway is needed for that kind of aircrafts. On the positive side, however, fixed-wing aircraft require much less energy to maintain their position, when already in the air.

Rotary-wing aircrafts, on the contrast, can generate sufficient lift from stand-still by adjusting the speed and AOA of the airfoils of the rotor. This process is called hovering and requires a lot of energy. Thus, although the rotary-wing aircrafts have less requirements in regard to the take-off and landing location, their range of flight is vastly limited.

It should also be mentioned that most rotary-wing aircrafts (e.g., helicopters) require additional tail rotors to prevent the rotation of the fuselage along the yaw axis (see Figure 1.2). On the multi-rotor rotary-wing aircrafts (e.g., drones) this problem is solved by compensating torque, generated by one rotor, with the torque of other rotor(s), which is rotating in the opposite direction. [2]

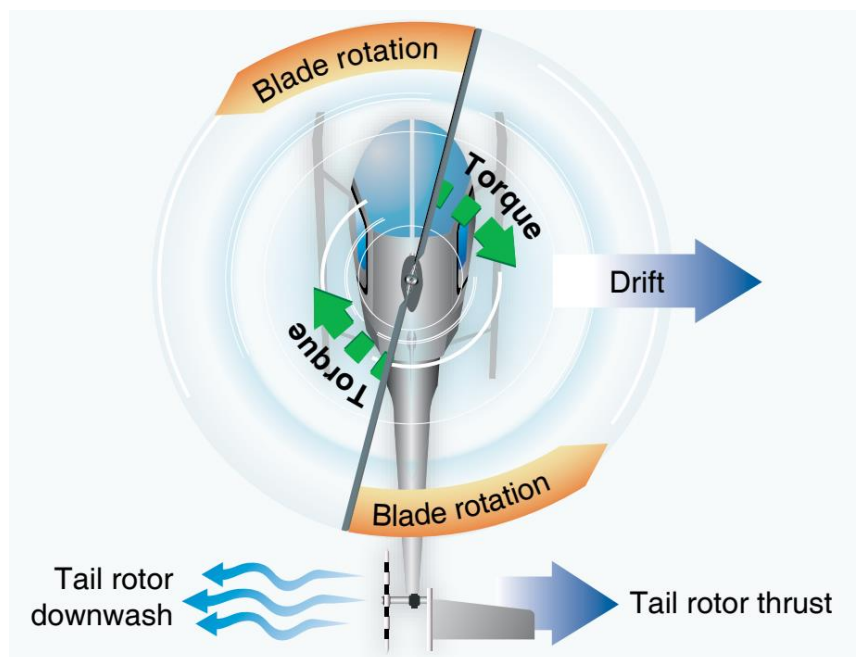


Figure 1.2 Function of the tail rotor in the helicopter [2]

Looking at those advantages and disadvantages of main aircraft types a question arose: Will it be possible to create a new type of aircraft, which will combine hovering during the take-off with a more energy-efficient fixed-wing-like flight in the later stages? Development of the Vertical Take-Off and Landing (VTOL) aircrafts in the middle of the 20th century were an answer to that question.

Currently there are 3 main concepts of the VTOL Unmanned Air Vehicles (UAVs):

- Tiltrotor (moving of the rotors relatively to fuselage)
- Tiltwing (moving of the wings relatively to fuselage)
- Tail-sitter (take-off from the position of sitting on the tail)

While first two concepts require a tilting of the rotors or wings, correspondingly, during the transfer from hovering to the forward flight, additional motors and/or gears are needed for these maneuvers. This results in additional wear of the mechanical parts and additional weight of the aircraft, what is especially crucial for the small UAVs. [3] [4]

Tail-sitter aircrafts provide a suitable alternative to the previous concepts in this regard, as no major moving parts of the aircrafts body are assumed here. Rather, the whole aircraft frame is tilted during the transition between forward flight and hovering mode. The first ever manned VTOL, Lockheed XFV -1 (see Figure 1.3), was a tail-sitter VTOL as well.

The main problem with usage of this concept back in the middle of the 20th century was the limited visibility from the cockpit. In the context of the UAVs, however, that is not a problem anymore. In addition, although the hovering efficiency of the tail-sitter VTOLs is lower than of the tiltrotor and tiltwing aircrafts due to the large, exposed surface area of a fuselage (especially true for flying-wing UAVs), their forward flight capabilities are supreme. [3] [4]



Figure 1.3 Lockheed XFV-1 VTOL [5]

Thus, it can be concluded that while diverse types of UAVs become ubiquitous in the modern world, tail-sitter VTOL aircrafts become more attractive in the light of the increasing importance of the energy efficiency and the range of flight. Modern engine concepts and control algorithms, described in detail in this work, could be aimed at achieving those goals.

The second chapter of the thesis concerns with the currently available VTOL engine solutions, control algorithms and mathematical models, whereby EDF motors are kept in focus. In third chapter the process of creation of a mathematical model for the tandem EDF motor system is discussed. The fourth chapter focuses on the experiments, conducted in order to acquire all of the physical characteristics of an EDF engine, needed for its accurate representation in the form of a mathematical model. The results of the whole work are described in combination with the possible upcoming steps in the closing chapter.

2. LITERATURE REVIEW

2.1 Different designs of VTOL UAVs

Diverse types of aircraft construction are in use for unmanned VTOL solution. Different mechanical structures are preferred depending on the use of the UAV, but also location, number, and type of the engines. It shall be highlighted, however, that differences between the transition phase of VTOL aircrafts also have an influence on their construction.

Thus, the following sections will look at different engineering solutions used in each of the VTOL types, described in the Introduction section. This chapter focuses on the academic research-product prototypes, as there are not so many commercial VTOL UAVs and the details of their construction and control are not so well documented in the public field [4].

Due to its less complicated constructions, it is possible to operate a **tail-sitter VTOL** with only one rotor. Example of such solution could be found in the lightweight drones with rigid wing-fuselage design and a single unprotected propeller in the front (see Figure 2.1). This design was popular in the early days of the VTOL UAVs thanks to its apparent simplicity. This simplicity of mechanical design, however, results in a great strain on the controllability of the aircraft. [6] [7]



Figure 2.1 Tail-sitter with a Single Thrust-Vector Propeller [6]

In addition to single-motor solution, wing-fuselage design UAVs with bigger number of motors were also developed and examined. In this applications, unprotected rotos are placed symmetrically on the wings and/or the tail, rather than in the front of the VTOL. Not only maneuverability and efficiency grow with the number of implemented motors, but also the weight of the air vehicle and complexity of its control. Lower number of scientific articles on the topic of wing-fuselage design UAVs with two rotors on the wings during last 15 years indicated a loss of their popularity [4]. Solutions with six rotors, on the other hand, are discussed only on the level of simulations [8].

Another widely used single motor solution for the tail-sitter is an Electric Ducted Fan (EDF), located in the tail of the UAV. EDF provides more up-to 21% more thrust, compared to the electric rotors without a duct. This increased energy-efficiency, however, comes in a cost of stability of the vehicle. Thus, this type of UAVs requires additional control surfaces (control vanes) which help to stabilize vehicle, especially during hovering. [9] [10]

One more simplistic design of the tail-sitter VTOL is called "flying-wing" (see Figure 2.2) and can be equipped with 2 or 4 motors, symmetrically placed on the edges of a single wing. This motors, providing a lift force during hovering and thrust during forward flight, can be controlled to balance each-other, whereby the quadrotor solution increases the stability of the UAV by mitigating aerodynamic interference between the wing and propeller.

Additional control of the course is provided by elevons on the bottom of the wing, which can be adjusted in order to change the AOA of the wing during the forward flight. Usage of elevons makes the UAV more efficient in the forward flight, especially for the 2-rotor construction, but makes the require control algorithms more sophisticated. [11] [12] [13]

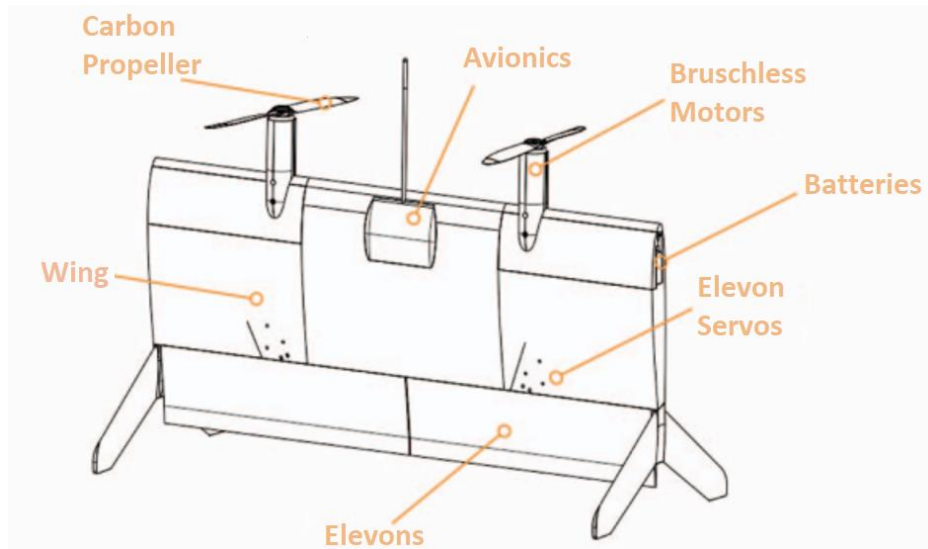


Figure 2.2 Hardware configuration of the Wingtra S100 [11]

By achieving superb differential rotor-thrust control with four independent rotors, additional moving parts of the flying-wing UAVs (e.g., elevons) can be dropped altogether. Those VTOLs usually have thicker middle part of the wing and rotors protruding into both directions from the main surface of the wing (see Figure 2.3). Flying-wing UAVs without control surfaces, as they are called, require sophisticated control algorithms but allow more robustness and possess a fantastic opportunity for various usages. [14] [15]



Figure 2.3 The Hong Hu quadrotor tail-sitter UAV [15]

Tiltrotor VTOL construction are distinguished by the location of wing and tail rotors. The simplest and oldest of the tiltrotor UAVs designs is the one with the two rotors mounted on the tip of the wing. Those rotors would tilt during the transition between hovering and forward flight, making more complicated actuation mechanism necessary.



Figure 2.4 Experimental tiltrotor aircraft with 2 propellers on the wings [16]

One of the great disadvantages of these early tiltrotor VTOLs with two propellers is the negative wash during the hovering phase, as part of the wing is located right beneath the propeller (see Figure 2.4). In addition, heavy rotors on the tips of the wings result in a shorter and thicker wing design, which influences the forward-flights capabilities of the tiltrotor UAVs negatively. [4] [16] [17]

By implementing four rotation propellers symmetrically around the center of gravity of the UAV (and directly on the wings) many of the problems of the two-rotor-solution, mentioned above, can be mitigated. Such design, however, makes the construction and actuation of the motors more complicated. In addition, it has certain efficiency disadvantages during the forward-flight, as rotors are located pairwise on one axis after tilting. [4] [18]

To increase the operability of the tiltrotor VTOLs with two rotors additional third rotor can be added on the tale. This helicopter-like tri-rotor solution provides additional thrust during tale-off and landing, as well as hovering phase. Solutions with fixed [19] and tilting tail [20] rotor are distinguished.

In case of a **tiltwing aircraft**, the whole wing of the of the aircraft should be tilted during the transition between different flight phases. As such wing construction helps to avoid negative wash of the motors, present in the tiltrotor VTOLs. In addition, fixed location of the rotors helps to optimize them for more efficient forward flight.

As the tiltrotor aircrafts, however, tiltwing UAVs require additional actuation and control set for the wing tilting, which results in the more complicated construction of the aircrafts. On the other hand, similar to the tail-sitter VTOLs, tiltwing aircrafts have less stability during hovering due to the large, exposed area of the wings.

Most of the tiltwing UAVs, described in the scientific literature, have two sets of tilting wings at front and back (see Figure 2.5). Such construction with four independent rotors symmetrically placed further from the center of gravity is similar to the common drones and provides thus superb hovering efficiency and control. On the other hand, additional pair of wings increases the weight of the air vehicle and the demand on its actuators. [21]



Figure 2.5 Accelerating transition of a tiltwing VTOL with 2 pair of wings [21]

Less popular are construction with 2 or 4 rotors on the wings and a tail rotor. Smaller popularity, compared to the tandem-wing constructions described above, can be explained by the tail rotor design. This motor is usually heavier and more complicated in control, compared to the common wing rotors. [21] [22]

2.2 EDF motor applications in UAVs

EDF motors are widely used for the UAV applications thanks to their higher thrust and higher efficiency for comparably small size, especially at the higher speed. In addition, ducting of the fan makes such engines safer and decreases their noise pollution. [17] [23] [24]

On the other hand, some of the drawbacks, such as high energy consumption, motor-generated angular momentum and vortex footprint are also typical for the EDF motors. In addition, housing around the motor adds weight and increases parasite drag. [17]

While the advantages of the EDF engines make them perfects for the UAV application, distinctive design solutions have been proposed over the years to tackle the disadvantages. Following sections of this chapter describe specific EDF powered construction and discuss their pros and cons.

As already discussed in Chapter 2.1, **single EDF motors** can be used in the tail-sitter VTOL applications [9] [10]. In those UAVs the control vanes (c1 and c2 on a Figure 2.6) are used unare used to compensate main shortcoming of the EDF motors – stability. Thus, the upper layer of the flaps (c1) in the model from the [10] is used to counteract the aerodynamic torque of the fan and control the yaw motions of the VTOL. Independent flips of the c2 level, on the other hand, change their AOA to control the roll and pitch attitude dynamics.

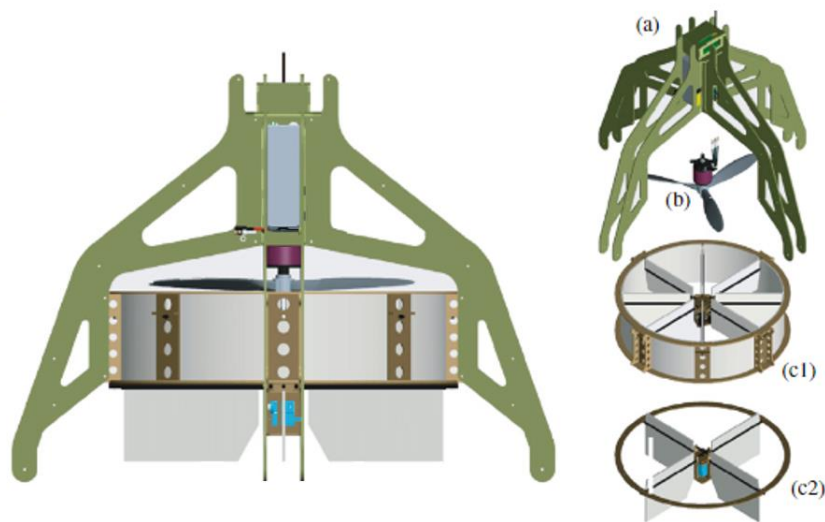


Figure 2.6 The ducted-fan micro-aerial vehicle with its sub-systems, a – frame, b – propeller and c1/c2 – control vanes [10]

It can be concluded that despite its simple mechanical construction VTOLs with a single EDF motor have comparably high requirements on the control level. Systems are equipped with a substantial number of sensors, sophisticated control algorithms and additional mechanical actuators [10]. Thus, a high dependency on many varied factors possesses a question of robustness of this kind of solutions.

To overcome stability issues, coming from the usage of the EDF motors, more complicated **VTOL construction with two separate EDF motors** have been proposed. These solutions provide simpler and more robust control over the air vehicle, by compensating the forces by adjusting the speed of separate fans. This requires, on the downside, bulkier, heavier, and more expensive mechanical constructions.

In [25], for example, a UAV with two separate EDF motors, although not a VTOL, is examined (see Figure 2.7). Rotation speed difference between front and rear motors allows to control the aircraft dynamics over the pitch axis, while changes in blade angle (cyclic pitch system) is used to control the roll axis. As each of the separate EDF motors has two rotors (upper and lower), rotating in different direction, control over yaw axis is also achieved.

A low order control algorithm is used to apply all of those separate control mechanisms during the flight. The authors of [25] conclude that although their control system performs well, additional work needs to be done to integrate speed and position control into it. It should also be noted that no tests on the actual UAV have been performed during this work.

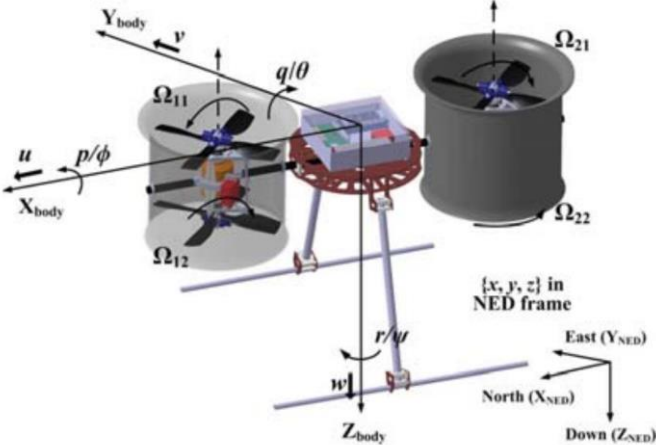


Figure 2.7 Model of a dual EDF motor UAV [25]

It should be added that some mechanically more complicated manned VTOL concepts with 4 separate EDF motors are also presented in the literature. In [26], for example, authors discuss a concept design for an urban air mobility vehicle for 4-5 passengers. VTOL construction with four separate EDF motors fits such purpose well, as robustness and stability of the control are the key parameters for applications involving humans. Cost of the vehicle, on the other hand, does not play such a crucial role as in the field of UAVs.

Tandem EDF construction for the VTOL application implies powering an UAV with counterrotating EDF motors placed on the same axis. Such compact placement of the motors would help to stay in the same small form-factor as the single-EDF-motor UAV solutions, described in Chapter 2.1 with increased thrust (up to 84% of sum of separate EDF motors) and efficiency (up to 16%). Clever control tactic of tandem EDF would also help to eliminate vortex footprint and angular momentum, inherent in the single EDF motors. [27]

The author of [28] proposes a VTOL design for purposes of academic research. Two counterrotating EDF motors with rotors attached to each are placed along the Z-axis of the UAV, similar to the solution discussed during this work. Due to the specifics of the construction, however, only differently sized rotors could be attached to the EDFs. As a result, most of the parasitic dynamics of the single EDF cannot be cancelled and a row of additional control surfaces – 12 flaps at the tail of the air vehicle – are required. Outer shape of the vehicle is used as a duct.

In another research [29] authors proposed so-called Double Propeller Ducted-Fan (DPDF) design for a VTOL used for infrastructure inspection and human interaction. In the paper it is claimed that counterrotating EDFs in their model can help to cancel out the effects of the gyroscopic precession torque of the single motors and thus enable the control of the yaw dynamics. Thus, only a one level of the flap is needed to stabilize the flight. Authors have performed simulations and have gotten promising results. Yet, as it was the case with the previously described work, physical prototype is still to be obtained and evaluated.

On a contrast, Tõivo Nerep [17] has concentrated his efforts during a Master Thesis on construction of a working prototype of a tandem EDF tail-sitting VTOL and testing of its performance of the test bench (see Figure 2.8). Yaw dynamics of the VTOL, on which the present work is based, are controlled purely by the EDF motors. For an overreaching control of pitch and roll axis additional control surfaces with the corresponding servo actuators were placed in the tail of the VTOL.

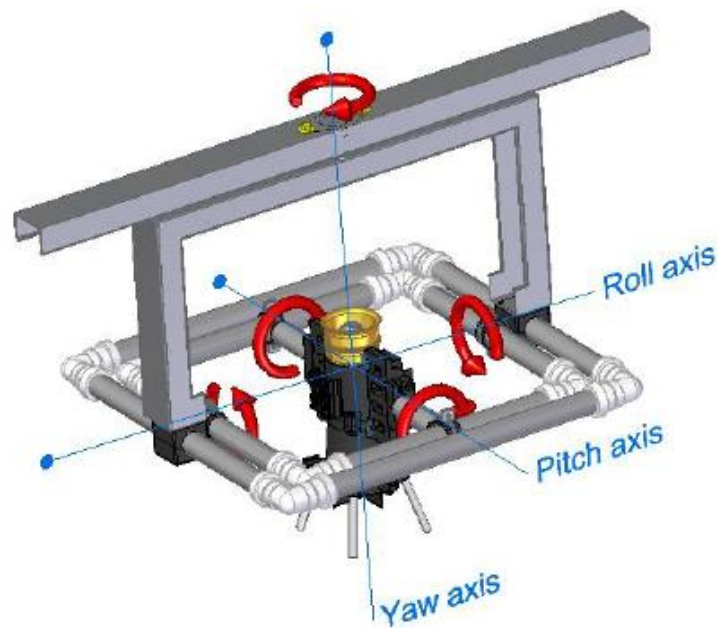


Figure 2.8 Tandem EDF VTOL in the test bench [17]

Although there is still some room for improvement, conclusions of the work were promising. Physical tests on the test bench showed, that counterrotating EDFs are able to cancel gyroscopic effects so well, that only two separate PID controllers for control surfaces in the tale were needed for the hovering phase. Still, more studies and design adjustments (e.g., adding of the wings for the forward-flight) are required to cover the transition and forward-flight phase of the VTOL operations to acquire a fuller picture.

2.3 Control algorithms for VTOLs

During hovering, transition, and the forward flight a VTOL aircraft faces different challenges and obstacles, as the environment changes together with the special position of its rotors. Thus, for this type of aircraft, control task possesses one of the main barriers on its way to the global market.

One of the main factors, making a creation of an overreaching control for the VTOL UAVs, is the nonlinearity of it flight dynamics. This is especially true for the transition between hovering and forward-flight or vice-versa, although some nonlinearities are present at each stage of the flight. Thus, classical solution for that control problem in the aviation –

linearization around single working point – would not yield a good result for the VTOLS. [4]

Keeping this in mind, Scheduled Control Approach can deal as an alternative to Unified Control Approach in the VTOL applications. During Scheduled Control Approach the whole flight dynamics are divided into finite number of independent sets (trim-points) and linearized. Then, separate control algorithms solve individual problems providing a supreme effectiveness on the curtain set. These control algorithms will be turned on-and-off during the flight, as the aspects of the flight (e.g., speed, altitude, flight-phase etc.) change, while only one controller for particular parameter is running at the time. [4] [17]

Given chapter give an example of different control methods application in the VTOL control algorithms, with the focus on tail-sitter solutions.

PID controllers are most widely used controller types and VTOL applications are not an exemption. For a PID control, which stands for Proportional, Integral and Derivative, its output $u(t)$ can be described as a function of an error $e(t)$ (difference between the set point and the measured value) as follows [30]:

$$u(t) = K_p e(t) + K_I \int_0^t e(t) dt + K_D \frac{de(t)}{dt} \quad (2.1)$$

Coefficients K_p , K_I and K_D are called proportional, integral, and derivative gains accordingly and can be adjusted during the process called tuning. Goal of the tuning and is to decrease the error $e(t)$ as fast and as much as possible, while trying to limit the overshoot (increase of the control value over the set point) as much as possible.

As it is obvious from the Equation 2.1 – no system model is required for the PID control. This is one of the main reasons, why PID controllers are so popular among engineers – acceptable control over the system can be achieved without really knowing all of its parameters. On the other hand, PID controllers require reliable and fast information from the sensors to work accurately. In addition, some complications with the non-linear systems are to be expected. [17] [30] [31]

One example of a such approach is to be seen in [9], in which the authors of a tail-sitter VTOL with a single EDF motors, described in Chapter 2.2, have chosen to use a PID controller for hovering flight maneuvers. Here, the desired VTOL coordinates are compared with the actual ones and sent into the first layer of PID controller (see Figure 2.9). Output

of those PIDs, velocity signals, are transformed into the velocities of the body attached frame using measured Euler angles and a rotation matrix. These are once again compared to the actual velocities in all three direction and sent into the 2nd layer of the PID controllers. Finally, saturated reference values for the pitch and roll are sent to the Inner PID controller which calculates corresponding AOAs (α_x and α_y) of the flaps, while saturated value initially coming from the altitude reference signal is used directly to control thrust (T).

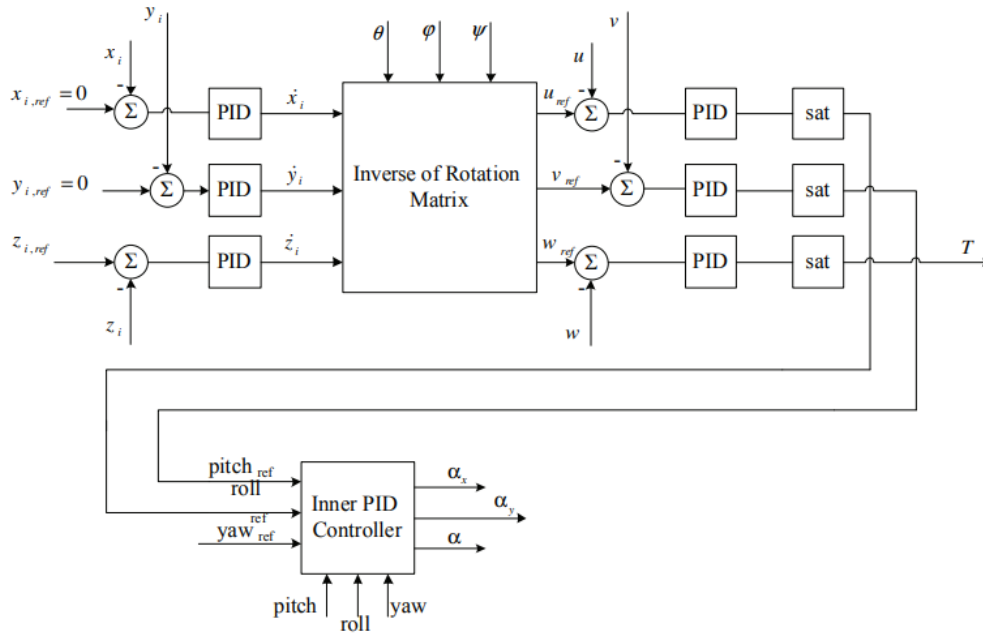


Figure 2.9 Block diagram of proposed PID Controller [9]

The number of PID controllers, used in [9], highlights additional disadvantage of this type of the controls – each variable requires its own controller. With that being said, described system showed satisfactory results and a great robustness with regards to the weight of the VTOL during the simulations described in article.

Linear Quadratic Regulators (LQR) is based on the linearized controlled system model representation of the following form [4]:

$$\begin{cases} \dot{x} = Ax + Bu \\ u = -Kx \end{cases} \quad (2.2)$$

Output gain matrix K , in this case, optimizes the closed-loop system with a cost-function, depending in the error and input weighting coefficients. As the parameters of the system changed significantly during various stages of the flight, similar to the PID control, LQE control in the VTOLs usually requires a Scheduled Control Approach. [4]

Although being known as robust, LQR depends heavily on the quality of the model and absence of any big disturbances. Authors of [32] have found, for example, that comparable results can be achieved by model-based scheduled-LQR and model-free PID Control. Thus, the future of more complicated LQE approach doesn't seem to be very promising.

Robust Control are controlling approaches, which aims on utilizing linear control techniques during the whole duration of the VTOL flight by making the control algorithm robust to the changes in the environment. This is usually achieved with the help of some additional modifications in the control structure. [4]

Authors of [33] have concentrated on the highly non-linear transition maneuver of the tail-sitter VTOLs to evaluate their robust control approach. Control task is divided into speed channel (certain minimal speed needs to be achieved to begin of the forward-flight phase) and attitude channel (control of the fuselage rotation mainly through the pitch axis). To aid the linear control laws, described in the article, values of some of the parameters are adjusted in accordance with the system variables. Figure 2.10, for example, shows a map with pre-calculated value of thrust as the function of forward and rotational speed. Usage of the prepared map (combined from various sources for that particular application), rather than the separate equations, helps to keep the calculations fast and simple.

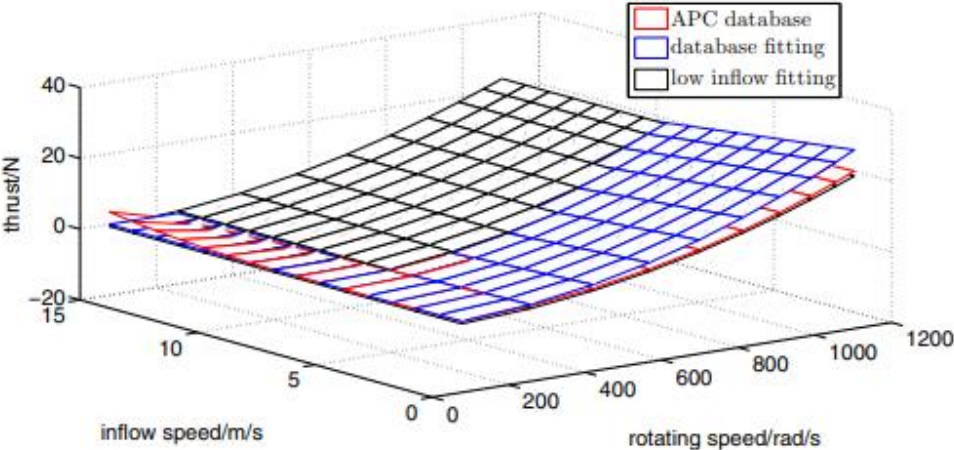


Figure 2.10 Mapping technique, used to recalculate the parameters for the robust control law [33]

In [34], on the other hand, so-called "Flight Planner", an external maneuver generator, is used to calculate the references for the PID control. Although the usage of external

calculations increases the demand on the quality of the system models, used for that, successful results from the articles described in this chapter can not be ignored.

Model Reference Adaptive Control (MRAC) is based on the estimation and recalculation (θ) of the parameters of the given control law by the means of comparison between the reference mode (y_m) and real output (y) (see Figure 2.11, with r being an input and u a control signal). MRAC allows to control the VTOL during the whole duration of the flight even by simple linear controllers like PID or LQR at the expense of a bigger number of real-time calculations. [4]

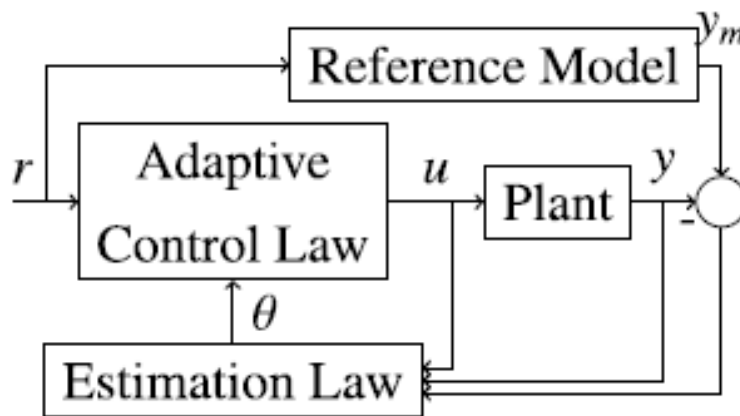


Figure 2.11 Block diagram of the adaptive control architecture [4]

In [35] a control method of an attitude dynamics of a twin-rotor tail-sitter UAV is discussed. Authors use MRAC on the top of the LQE to get more precise model of the pitch channel in the vertical flight mode by reducing the influence of large-angle attitude maneuver and other uncertainties.

For this purpose, a LQE system model is enhanced with a term, responsible for an output error. The adaptive control input is then calculated in a way that makes this error term as small as possible. Simulations prove the assumption that the error term will guide the system back into stability even if the variables will push it away from the linearized working point. [35]

One of alternative control algorithms, **reinforced learning**, is a model-free approach, which uses Neural Networks (NN) to train a VTOL dynamics controller. In general, NN is a structure consisting of separate nodes, neurons, which are grouped in layers and connected with each other (see Figure 2.12). Each of these neurons has a specific weight and a

threshold value. If and only if the threshold value of the specific node is exceeded, it sends its input data multiplied with its weight to the next node. [36]

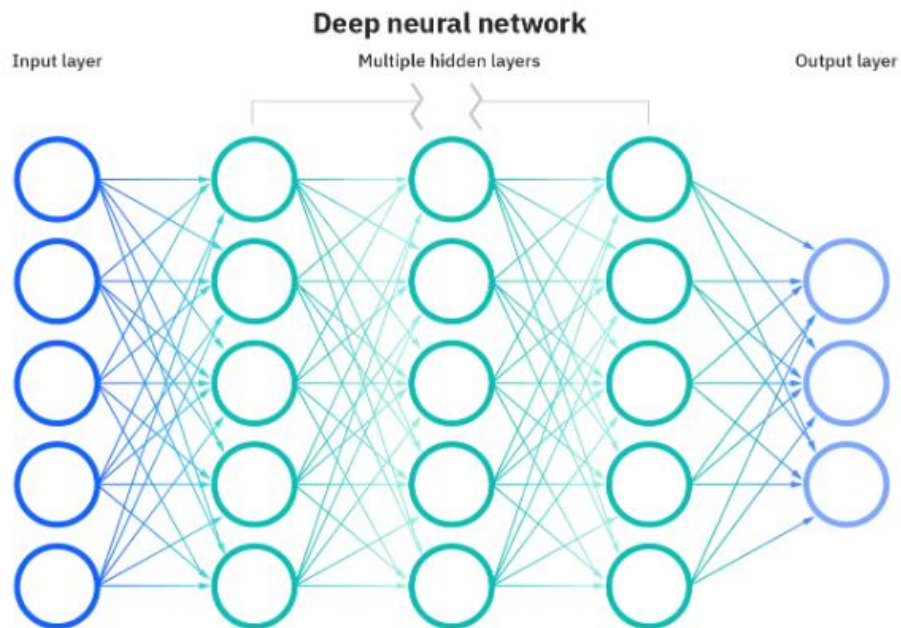


Figure 2.12 General structure of a NN [36]

In the case of the VTOL applications the input layer can be fed with the sensor data, while output layer of the NN should give the control values for different actuators. During the training period of the NN, which requires a rich input-output data of the system, node weights and thresholds are defined to perform the given control task as accurate as possible.

Measured data inputs are fed into the NN, outputs of the NN are then calculated and compared with the corresponding measured outputs. The algorithm gets “rewarded” for smaller errors and “punished” for bigger. The node parameters are then adjusted to yield a better result (smaller cumulative error) for the next iteration and the process continues until desired precision is achieved.

Authors of [37] have used velocity tracking error, energy efficiency, flight stability, error integral and vehicle orientation as the parameters to assess the efficiency of training algorithm. NN training was performed purely by using simulation data and no manual tweaking of the control algorithm has been made. Three distinct types of the VTOL aircrafts (tail-sitter included) were able to fly and successfully transit between the hovering and forward flight using the algorithms developed during described work.

Reinforced learning is a powerful tool for a unified control approach of the UAVs. The main issue with the NN training process is a need for a diverse and rich training data, covering all of the possible maneuvers and flight modes of the aircraft. Real-world data is not always available in the initial stages of the UAV design process and creation of trustworthy simulation data still required a precise mathematical model of the vehicle.

2.4 Mathematical models of VTOL UAVs

As the main goal of the thesis on hand is to create a mathematical model to the tail-sitter VTOL UAV described in [17], this chapter will focus on the challenges, requirements, and examples of a development of such model. Details of such models, together with the corresponding physical and mathematical equations, will be described in the Chapter 3 later in this work.

There is a huge body of research behind the mathematical models for dedicated forward-flight air vehicles. These classical models are analytical and are usually derived from the Newton's law or experimental data (e.g., wind-tunnel trials). Unfortunately, most of those models are not applicable to the VTOL aircraft due their linear nature and/or tight limitations of the parameters, rapidly changing during the transition phase of the VTOL (AOA, speed, etc.). [4]

Thus, as it was repeatedly mentioned in the articles used for this literature review, creating of the application specific VTOL mathematical model can be challenging and requires understanding of the aerodynamical effects and the variable limitations. This stays as one of the main motivations of writing the work on hand, which will center around the creation of comprehensive mathematical model for the hovering phase of the tandem-EDF tail-sitter VTOL described in the [17], with its subsequent verification on the test bench with a real-world model.

For the VTOL application, a fixed earth-based Inertial Frame with X_i pointing to the North, Y_i to the East and Z_i to the center of the earth is used, \mathcal{I} (see Equation 2.3). At the same time some of the equation described below require a vehicle-based coordinate system \mathcal{B} (see Equation 2.3) which has its origin in the center of mass (G) of the vehicle. Thus, it should be clearly distinguished between those two during the model creation (see Figure 2.13). Transformation between those two is performed using a rotation matrix, combining roll φ , pitch θ and yaw ψ angles of the aircraft.

$$\begin{cases} \mathcal{J} = \{O, \vec{i}_i, \vec{j}_i, \vec{k}_i\} \\ \mathcal{B} = \{G, \vec{i}_b, \vec{j}_b, \vec{k}_b\} \end{cases} \quad (2.3)$$

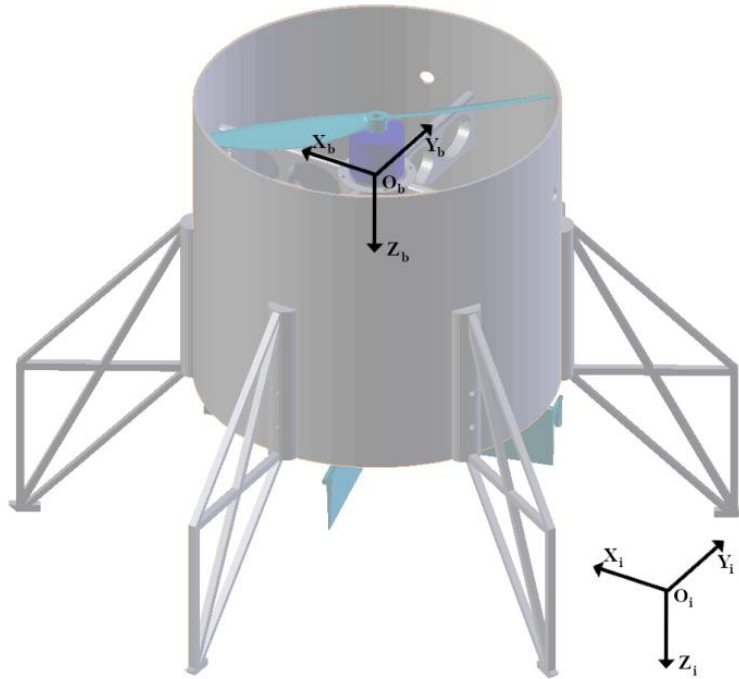


Figure 2.13 3D CAD of double propeller Ducted-Fan with the visualized Inertial and Body coordinate frames [29]

At the next step, Newton-Euler equation for a system with 6 Degrees of Freedom (DoF) should be set up. These equations describe the total force ($m\ddot{x} = \sum_{j=0}^n F_j$) and total torque ($I\dot{\omega} = \sum_{j=0}^n \tau_j$) applied to the air vehicle with m being the mass and I diagonal inertia matrix. Individual terms, which are the components of Newton-Euler equations, will be discussed in the Chapter 3.

To complete the model of the system, equations of motions should be written and examined. These mathematical expressions describe kinematical and dynamical behavior of the UAV and show the dependencies between the variables. Equations of motion will be then set-in the Newton-Euler equations, described in the previous chapter, to complete the mathematical model of the system. [4] [29]

2.5 Conclusion of the Literature Reviews

As the Literature Review shows, most complicated part of the mathematical model creation is the right assessment of the limitations and disturbances. In addition to the usual physical limitations of the output variables (e.g., engine thrust limitation) certain parameters should be met in order to maintain stable speed and orientation between, but also during various phases of the VTOL flights.

An example of such requirement is described in [33], as there are minimal speed requirements to the forward-flight phase of the flight. As was described in the Chapter 1, lift of the aircraft wings in the forward-flight is a function of AOA and the speed. Thus, if the required speed wouldn't be achieved at the beginning of this phase, VTOL in question will collapse.

This and other (e.g., acceleration limitations due to sensitive equipment on board) limitations should be defined and applied to the mathematical model, before an accurate representation of the real-world aircraft can be achieved. Same can be said about the internal and external disturbances, such as the effect of the propeller wash on the airfoils and the weather conditions. [4]

3.VTOL MODEL CREATION

3.1 Basis of the Mathematical Model

It was decided to use MATLAB/Simulink environment for the creation of the mathematical model of the VTOL question. MATLAB was chosen due to its widespread use in the research ([9], [11], [24] etc.), intuitive approach to the model creation (interconnection between the logical block in Simulink) and compatibility with Solidworks [38] and drone firmware [39]. Transferring a 3D-model from Solidworks to MATLAB not only allows a supreme visualization of the control process but will also help to make the model more realistic. Information about the physical dimensions of the model, calculated in Solidworks, can also be used as an attempt to breach the gap between the real model of an aircraft and its representation in a form of a mathematical model.

For smooth and aligned work on the model, its visual representation with block diagram was created beforehand. The diagram on the Figure 3.1 represents the result of several iterations and has five main modules, which are to be simulated in MATLAB:

- **Actuators** – Transfer the control values from Flying code into speed changes of EDFs and position changes of control surfaces.
- **Airframe** – Considers all of the forces/moments (internal and external) acting on the aircraft and calculates its position change in the space as a result of those. **Sensors** sub-system measures the position of the aircraft in the space and report it to the Flying code.
- **Flying code** – Series of (PID) controllers that compares measured results with the goal values (e.g., altitude of the drone) and tries to eliminate the difference between those (error) by adjusting the values of the actuators.
- **Environment** – Makes the model more realistic by changing some of the physical variables with the changes of the aircrafts position in space (e.g., air pressure), adding some irregular disturbances (e.g., wind) and compromising the sensor results with the realistic levels of noise.
- **Visualization** – Combines a visual representation of interaction and movement of different VTOL parts based on adjusted Simscape multibody model.

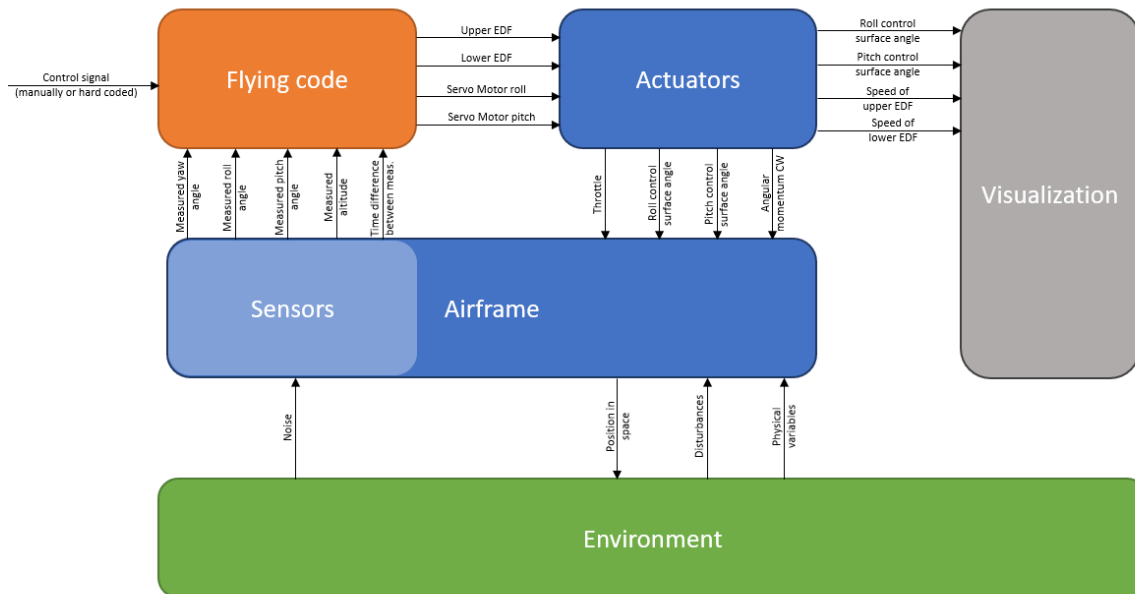


Figure 3.1 Block diagram of tandem EDF VTOL mathematical model

One of the other aspects of the block diagram on the Figure 3.1 are the connections between main modules, represented as arrows. Those connections, signals, help to highlight the main focus of the model on the initial stages of its development. In this particular case, for example, focus will lie on control of **yaw**, **roll** and **pitch angles** together with the **altitude** (Z-coordinate) of the aircraft. On the other hand, control aircrafts position relative to the earth surface (X- and Y-coordinates) will be excluded from this work as the tandem EDF VTOL in question lacks any reliable sensors for that purpose (e.g., GPS) [17].

It should be noted that aircraft coordinates in X- and Y-direction will be used to calculate a precise model of gravitational acceleration, as it changes with the latitude, longitude, and altitude. Corresponding calculations will be described in more precision in Chapter 3.3. Thus, the model itself could be rather easily extended to control all of the VTOLs coordinates in space if such need is to arise in the future.

Additional benefit of visual representation of the input/output relationship between the main modules of the model is a possibility to develop those modules independently from one another. It will ease usage of parallel development approach (when different developers work on parts of the model simultaneously), implementation of different model structures (Simscape Multibody will be used for the Airframe, but common Simulink blocks will be preferred for the Flying code) or independent deployment of the modules (Flying code could be applied to the microcontroller after implementation and verification inside of the mathematical model in MATLAB).

Following sub-chapters of Chapter 3 will describe structure of modules one-by-one and elaborate their connections with the real world tandem EDF VTOL model from [17]. Chapter 4 will discuss the experiments that have been performed in order to acquire physical characteristics of an EDF, required for its precise representation within the mathematical model.

3.2 Actuators

The Actuators module will concentrate on translating the control signals from Flying code into the real changes of the EDF motors speeds and the position of the roll/pitch control surfaces (actuated by two servo motors) on the tail of the aircraft. For that purpose, a deeper dive into the specifications of the motors in question will be required.

Two Dr. Mad Thrust 70 mm EDF motors are used as the main thrust sources in the tandem EDF VTOL in question. The one installed on the upper part of the airframe rotates counterclockwise (CCW) and will be called Upper EDF in the text below. The other fan with a clockwise (CW) rotational direction was installed on the lower part of the frame and will be called Lower EDF.

Maximal voltage level of Dr. Mad Thrust 70 mm is 14,8 V, which corresponds to the maximal thrust of the motor of 2,3 kg, at least according to the technical specification of the manufacturer. As to the Tõivo`s thesis, however, the combination of two engines can only achieve a combined throttle of roughly 2100 g [17]. Experiments, conducted as the part of given work, revealed even smaller numbers for maximal thrust on the motor – 0,527 kg per motor or around 1050 grams of thrust in total. That can be described by the underload of the EDF as a result of the frequency mismatch between electronic speed controller and the signal generator, see Chapter 4.2.

In scope of the given work, it was decided to go with the lowest, experimentally approved thrust numbers for the EDF. In order to calculate full thrust of the aircraft, input signals for lower and upper EDF have been firstly divided by 100% in order to enable calculations without the percentage in mind. Subsequently, Equation 4.3 (see Figure 3.2) has been applied separately to the lower and upper EDFs and the results have been summarized, resulting in an output signal from “Actuators” block with kilograms as a unit.

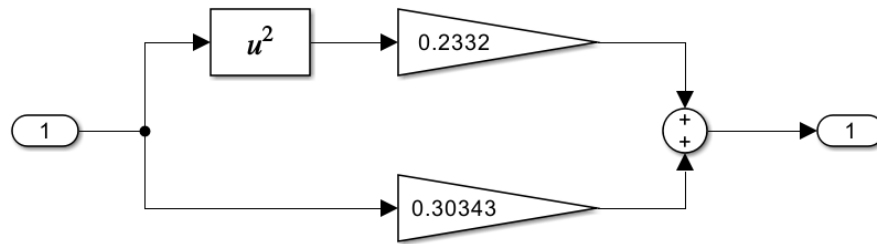


Figure 3.2 Application of Equation 4.3 for Thrust calculation in MATLAB/Simulink, with left "1" box representing an input (EDF power level), " u^2 " squaring, "0.2332" & "0.30343" multiplication with corresponding numbers (gain) and right "1" an output (thrust power) after addition of both paths (squared and linear)

Similar approach has also been taken for the calculation of the overall torque of the aircraft. Input signals, divided by 100%, were applied to the Equation 4.2 in order to obtain the angular momentum for individual engines. Those were then summarized, while the torque for the CCW engine has been applied with the negative sign. Thus, when the CW is rotating faster than the CCW, the "Actuators" block outputs positive torque and vice versa. That factor in particular would be used to control a yaw angel. As discussed in Chapter 4.3, Newton-meters are being used as the unit of torque during this work.

Lastly, speed of each of the motors was calculated, resulting in individual outputs in rotations per minute. Those outputs were calculated using the Equation 4.1 and supplied to the "Visualization" block to enable visual representation of the EDF rotation. This topic will be discussed in more detail in Chapter 3.6.

Some calculations have also been performed in scope of the "Actuators" block for the Corona CS - 239MG servo motors, as they were chosen for actuating roll and pitch control surfaces. Roll and Pitch control surfaces, which are set into motion by corresponding servo motors, are limited to the rotations of +/- 15 degrees to their nominal position straight down. Due to the reference points of those angles, chosen by Tõivo in his work, an offset of 80 degrees has been added [17]. This resulted in an output of a value between 65 and 95 degrees for both control surfaces.

3.3 Airframe

Airframe represents the calculation of VTOL body movements in space as a result of all forces and moments acting upon it. Instead of creating my own equations of motion, a block "6DOF (Euler Angles)" has been chosen from the Aerospace Blockset in Simulink for those purposes. This block implements the Euler angle representation of six-degrees-

of-freedom equations of motion, described in Chapter 2.4. The block in question gets sum of the forces and angular moments, acting upon the body of a VTOL at every moment, as an input and gives aircrafts position in space (coordinates, speed, and acceleration) as an output. [40]

It should be noted that realistic mass and inertia of the aircraft body in body fixed coordinate system have been measured in Solidworks and applied to the "6DOF (Euler Angles)" block in Simulink. All other initial conditions (e.g., positions of different axes) has been left untouched, representing an aircraft standing firmly on its landing gear, pointing straight up and ready to set off.

As a result of those initial conditions Flat Earth reference frame is identical with body-fixed axes and a rotational matrix between coordinate frames is a 3x3 Identity matrix (see Figure 3.3). When an aircraft starts moving, however, so does the body-fixed coordinate frame and the rotational matrix (DCM variable) is being updated with each new calculations cycle. This DCM matrix is then used to transform the external forces (e.g., gravity) from Flat Earth reference frame into the body-fixed coordinates. These forces are then summed up with the internal forces of the VTOL (e.g., thrust) and applied as an input to the "6DOF (Euler Angles)" functional block.

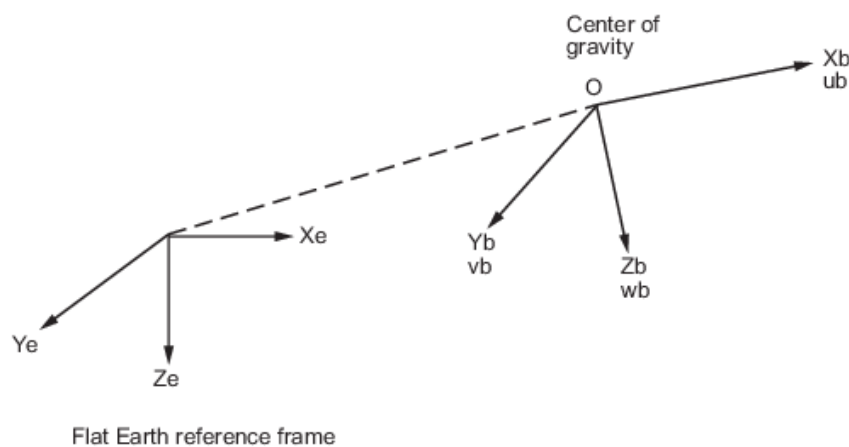


Figure 3.3 Coordinate frames used in "6DOF (Euler Angles)" block in Simulink [40], with X_e , Y_e and Z_e being the coordinates in Earth frame and X_b , Y_b , Z_b , u_b , v_b and w_b coordinates and corresponding speeds in Body frame

Thrust force is being calculated within the Airframe block by multiplying the results from Equation 3.1 with the gravitational acceleration. The same operation is done with the mass of the drone to get a gravitational force. For both of those purposes' gravitational acceleration, calculated based on latitude, longitude, and altitude in the Environment block (see Chapter 3.4), is being applied.

To calculate the forces, produced by movement of the Roll and Pitch control surfaces, an approach prevalent in the other segments of the avionics industry has been chosen. Similar to the calculation of lift based on the airfoil form and an AOA via lift coefficient (C_L) in the fixed-wing aircrafts [41], roll (C_R) and pitch (C_P) coefficients have been introduced into the model. Thus, the forces in X and Y direction in body-fixed coordinates of an aircraft have been calculating by multiplying a thrust force with a corresponding coefficient that is, in its turs, dependent on the angle of rotation of the related control surface.

As series of test in the wind tunnel to get accurate coefficients for roll and pitch would be required, what is out of scope of given work, approximate numbers from the literature have been chosen. Due to their uncomplicated form, control surfaces for roll and pitch remind the symmetric airfoils (e.g., NACA 0012) with rather linear characteristics between AOA of -15 degrees to 15 degrees (see Figure 3.4).

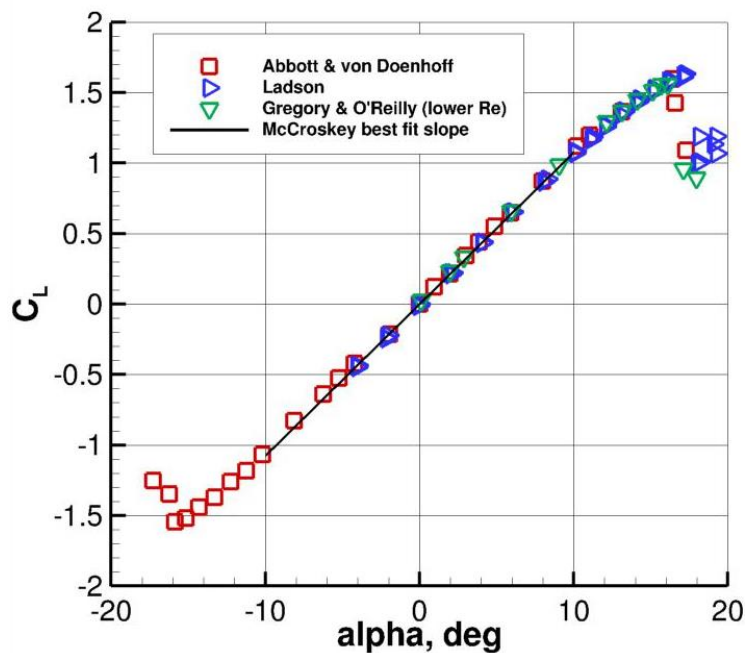


Figure 3.4 Lift curve for NACA 0012 airfoil with C_L as a lift coefficient, alpha as AOA, colorful triangles and squares representing different experimental dataset and a black line being the best fit for all given experiments [42]

As in tandem EDF VTOL, which is being discussed in the course of this work, the movement of control surfaces is limited within the same values, it was decided to equate C_R and C_P with C_L from the NACA 0012 airfoil. Thus, an increase of control surface angle of 1 degree will result in increase of corresponding side forces of additional 10% of the thrust force, generated by the EDF motors. [42]

It should have been noted, however, that some studies (e.g., [43]) show that a linear increase in the lift coefficients for NACA 0012 airfoils stalls before the value of AOA of 15 degrees. In addition, strong relation between the coefficient and the Reynold`s number has been reported [43]. Despite those findings` linear simplification of roll and pitch coefficients is deemed to be sufficient for the stated purposes of this work. More detailed exploration of those numbers should be considered during the future studies.

In addition to the sum of forces, sum of torque values in the VTOL`s center of gravity deals as a second input to the "6DOF (Euler Angles)" functional block. Here, however, only internal torques has been taken into consideration, as it is assumed that all the external forces (e.g., wind, gravity) apply exactly to the center of gravity and thus, lacking a lever, does not generate any torque. This simplification is being considered, as the drone in the center of this work is mostly symmetrical and realistic small power levers would not alter the results of the calculations much.

In addition to the angular momentum of each of the EDF motors, described in the Chapter 3.2, torque due to the forces produced by roll and pitch surfaces on the bottom of the aircraft is being considered. There forces are multiplied with the distance between the middle of the corresponding control surface and the center of gravity on the aircraft and are seen as the main influencers of the roll and pitch angles in the model.

Values, describing the position in space (coordinates, Euler angles, DCM) are being used as the outputs of the "Airframe" block of the model. Other build-in outputs of the "6DOF (Euler Angles)" functional block (e.g., speed, angular acceleration) are currently being dismissed but can be used for future iterations of the model.

Lastly, "Sensor" sub-block of the model is built rather simple and has its main goal in introducing noise to the actual values describing the position of the VTOL in space. Here, the noise is added to the yaw, roll and pitch angle measurements, together with the altitude values acquired in the "Airframe" block.

Noise signal is an additional input to the block, while amplitude of the noise is adjusted for each specific signal by different gain values. Altered values of the controlled parameters deal as outputs of the block.

3.4 Environment

"Environment" block of the model consists of 3 outputs: gravitational acceleration, wind force and noise, while aircrafts real altitude and current rotational matrix are taken as

an input to the block. In addition, latitude, and longitude of my hometown of Tallinn (59.43696; 24.75353) are used as inputs for the gravitational acceleration. These geographical coordinates can be made dependent on the location of the aircraft or computer, the model is running on, in future updates of the model.

“WGS84” functional block in Simulink uses previously described coordinates in conjunction with the current altitude information from the VTOL to calculate actual gravitational acceleration, which affects the aircraft in the moment. This block uses mathematical representations of the World Geodetic System (WGS84) as its reference coordinate system [44]. This standard has been chosen due to its high precision and ease of implementation in Simulink environment.

Functional block in Simulink, responsible for calculation of gravitational acceleration in accordance with WGS84 standards, has a vector of gravitational accelerations in north-east-down (NED) coordinate system as an output [44]. To make the calculations simpler, only the most prevalent acceleration towards the middle of the Earth (down direction, 3rd component of the output vector) has been filtered out and used in the previously described calculations in Chapter 3.3.

It was decided to add some additional disturbances to the system in order to control robustness of the control algorithm. This was realized with an introduction of a wind model, based on a “Wind Shear Model” functional block in Simulink. This block takes the coordinates of an aircraft together with a latest rotational matrix (DCM) and gives mean wind speed vector in body-fixed coordinates as an output [45]. To get the wind forces from that speed, following formula was implemented [46]:

$$F_{wind} = \frac{1}{2} \cdot c_f \cdot A_{ref} \cdot \rho \cdot v_{wind}^2 \quad (3.2)$$

With:

- F_{ind} – Force of wind in particular direction
- c_f – Force coefficient based on the reference area A_{ref}
- ρ – Density of air
- v_{wind} – Speed of wind in particular direction
- A_{ref} – Surface area of an aircraft, facing the wind from particular direction

Calculations had been realized in the mathematical model by separating independent components of the velocity vector and putting those into square. Those were then multiplied with average air density during cited experiment ($1,22 \frac{kg}{m^3}$ [46]), approximate

surface area of the VTOL 3D-model projection onto the corresponding plane (taken from Solidworks) and divided by two. Force coefficient value (c_f) was chosen to be equal to 1 out of the simplification reasons. This can be justified by a fact, that wind forces are only applied as a disturbing factor for mathematical model in question and the precision of their absolute values is of a secondary importance. With that being said, this coefficient could also be measure in the wind tunnel test and introduced to the model.

Lastly, a "Band-Limited White Noise" functional block has been implemented for sensor noise generation, described in Chapter **Tõrge! Ei leia viiteallikat.**. Simulink block in question generates normally distributed random numbers, which makes it perfect for serving its purpose of "flickering" the sensor values [47].

3.5 Flying code

The "Flying code" block of the model comprises all of the controllers and is thought to be transferred into the drone if a need appears. Core of the block are four PID controllers that are in charge of all four measured values in the given system: yaw, roll and pitch angles, as well as altitude. In accordance with classical PID control loop structure, each of the PID controllers is comparing defined Set Value (SV) with a measured Process Value (PV) and reacts upon the difference (error) and its rate of change. Theory behind this control algorithm was described in Chapter 2.3.

Within the framework of mathematical model in question a continues-time and parallel PID controllers from the Simulink library have been implemented. Continues-time variant has been chosen due to the non-discrete definition of the model itself, while parallel PID, being defined as providing independent reaction of each of the PID sub-functions to the error, has been chosen due to its simpler tuning and real-world implementation experience.

Due to the high non-linearity of the model's build-in function of the PID controllers autotuning could not be implemented during this work. Thus, manual tuning with process of trial-and-error has been used to define the values of P, I and D for each of the controllers. Main goal of the tuning process was to provide stable and robust control (overshoot under 5% and no long-lasting oscillation) within the usual range of VTOL implementation (small tilt angles, altitude between 0 and 100 meters).

After the PID control output for each of the measured values has been defined, the signals are being transformed to serve as an input signal for each of the four previously

described electrical motors (two EDFs and two servos). For that purpose, all signals are limited in the different ranges. While pitch and roll PID controller outputs are limited between -100 and 100, representing the maximal movement of the corresponding servo motors to one or the other direction, calculations for EDF engines are slightly more complicated (see Figure 3.5).

For each of the independent EDF engines (upper and lower) 97,5% of the signal comes from the altitude PID controller. Thus, the output of the PID in question is limited between 0 and 97,5, as those engines are not designed to rotate in different direction. Additional 2,5% of power can be added or subtracted from each of the engines to enable the control of the yaw angle. For that purpose, outputs from the yaw PID controller are limited between -2,5 and 2,5 and supplied to different EDF engines with a different sign ("+" for the upper and "-" for the lower), resulting in a maximum of 5% different between power on the different motors. This variation in power will result in a different torque on the motors, consequentially rotating the body of the VTOL along the Z-axis and changing the yaw angle accordingly.

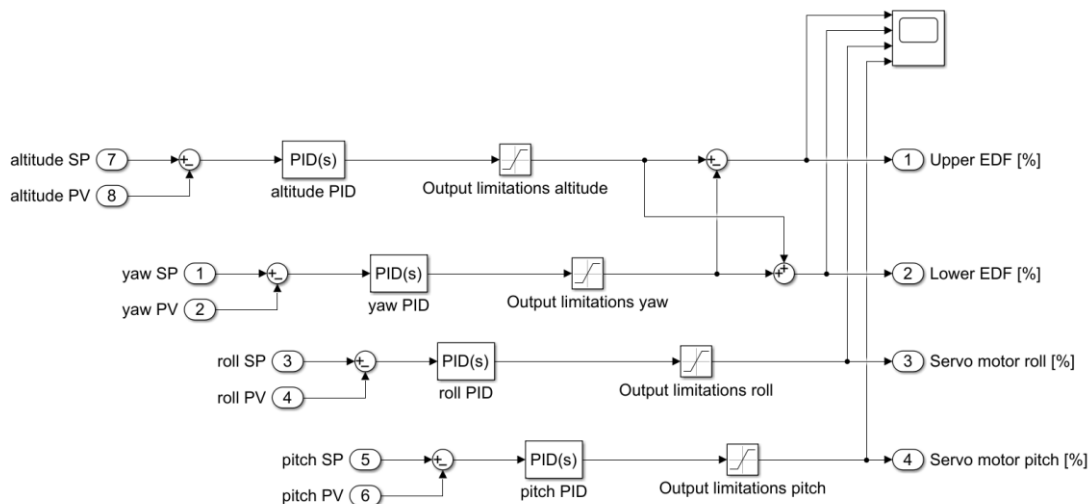


Figure 3.5 Flying code block

It should be noted that those calculations assume linear behavior of the engines as the thrust lost by slower EDF should be compensated by the faster one. This is not completely true, as the Chapter 4.3 suggests. Small error of such calculation can be, however, accepted within a limited range of power (+/- 2,5%) as its influence would be hardly noticeable. This simplification can be considered as a model improvement opportunity in the future implementations.

The results of the manual PID tuning for roll, pitch, and yaw angled can be seen on the Figure 3.6. For that particular case, Set Values were set manually to -10 and +15

degrees for roll and pitch, as well as +45 degrees for a yaw angle. The results show that acceptable control of those parameters is achievable in the framework of the given mathematical model and thus can be seen as successful.

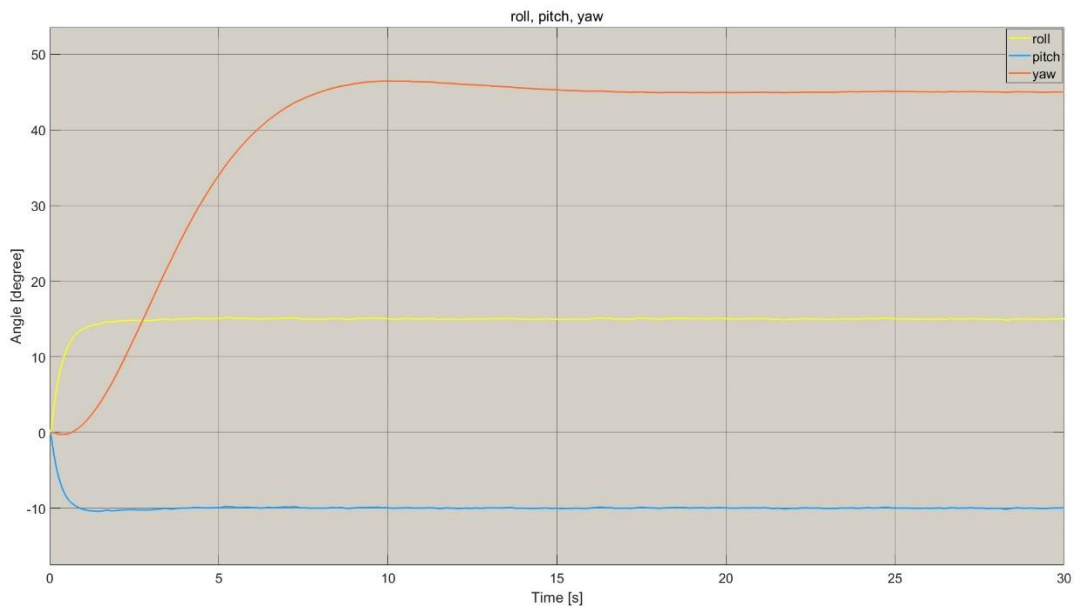


Figure 3.6 Roll, pitch, and yaw control results

Comparable results were also achieved for the altitude control, with 75 meters being a Set Value for the simulation, illustrated on the Figure 3.7. The VTOL showed no overshoot and very slight oscillations for the simulation in question, error after 30 seconds was around 0,35% (74,737 meter). This behavior of the model also proves that it can be made controllable using the PID logic.

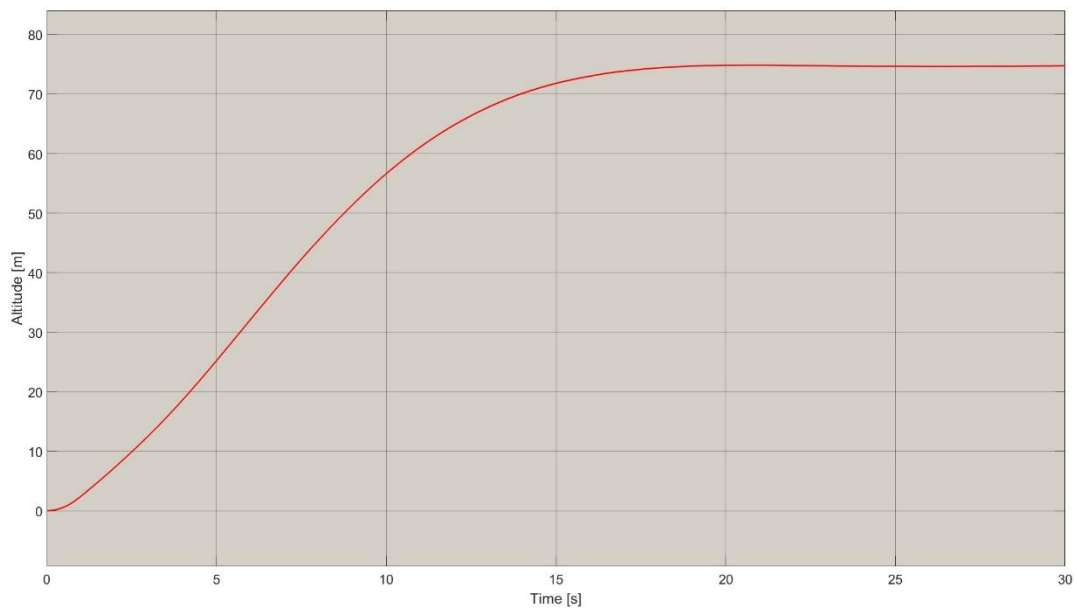


Figure 3.7 Altitude control results

3.6 Visualization

For the purposes of the aircraft visualization a 3D-model of the aircraft, created in Solidworks, was uploaded to MATLAB/Simulink. On the Simulink side, Simscape Multibody simulation environment was used. All VTOL parts have been uploaded to the environment as a separate entity (bodies) and the relationships between them were automatically copied from the 3D-modeling software. After that some cleaning, sorting, and adjusting work had to be done manually, as not all of the complicated relationship between parts are uploaded to the Simscape Multibody environment correctly.

After the preparation work only four parts have been allowed to execute rotational movements around some axis: both EDF motors as well as pitch and roll control surfaces. The system was supplied with four inputs, rotational speed in RPM for both EDF engines and the angles for the control surfaces. These physical values could then be represented as the movements of corresponding parts during the simulation (see Figure 3.8). Visualization of the VTOL mathematical model can deal as a mean to understand the processes happening during the simulations in a more graspable way than by looking through the abstraction of the graphs.

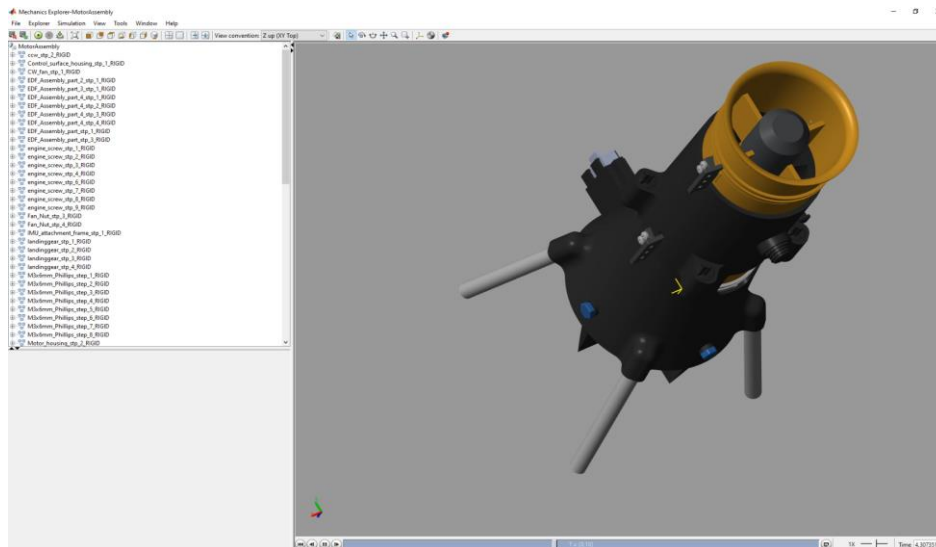


Figure 3.8 Simulation of the tandem EDF VTOL in a Simscape Multibody environment, with parts imported from Solidworks to be seen on the left side of the screen and the visual representation of the control mechanisms movement in the middle

Described feature can be perfected and used in conjunction with other graphical models (e.g., particular environment) to perform different maneuvers in the virtually, before their implementation on the real aircraft. This can help to reduce time and money spend during the Research and Development phase by reducing the number of actual hardware test and weeding out more dangerous ones.

4. EXPERIMENTS

As experiments with the thrust measurements of the fully assembled tandem EDF motors in question (see Figure 4.2) showed in [17], the technical characteristics provided by the supplier of the equipment could not be blindly trusted without verification. So, according to the mapping test experiments, combined power of two EDF motors from Dr. Mad Thrust could provide only 2093 grams of thrust at its peak. This is less than theoretical maximal thrust of a single EDF from that supplier, being stated as 2300 g in the specifications.

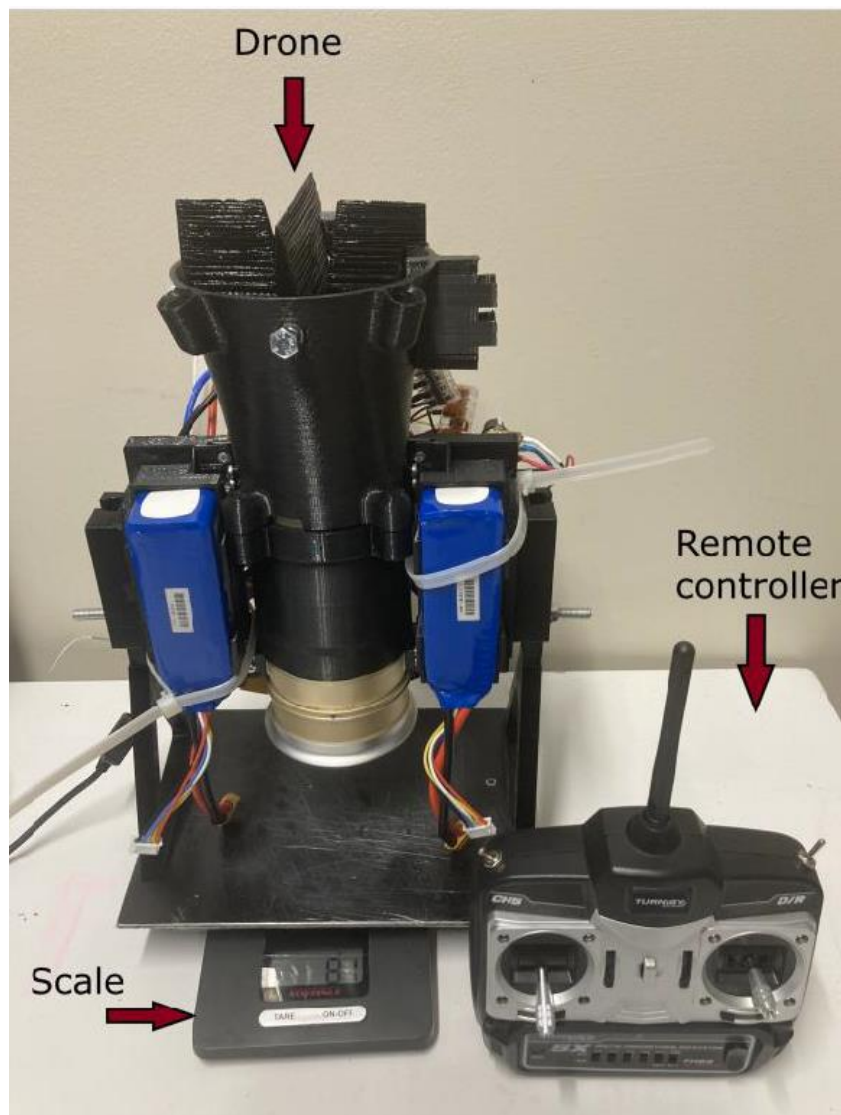


Figure 4.1 Throttle mapping test equipment used in [17]

In addition, not all of the values, needed for the realistic mathematical model of the tandem EDF VTOL in question, are available on the supplier's technical specifications datasheet (e.g., angular momentum). To determine the physical characteristics of the

given EDF motors a series of experiments has been conducted. The same equipment and procedure can be used in future to acquire comparable physical characteristics of different electrical motors. This is especially important as cheaper electrical motors from less renown brands are being used to bring the cost of the UAVs down.

4.1 Equipment and Process

An RCbenchmark Series 1580 test stand was used as a main measuring device during the experiments. This test stand was designed specifically for evaluation of brushless motor propulsion systems, like the one that is powering an EDF engine. RCbenchmark equipment, in addition to torque (angular momentum) and thrust, is being able to measure rotational speed of the motor, together with its power consumption and ambient temperature. [48]

An electrical motor under test was activated using a PWM signal from Rigol DG1022Z (max. frequency 25 MHZ) generated using a MATLAB code, that gradually increases the duty cycle of the PWM signal from 10% to 100%. The entire system was powered by TDK-Lambda Genesys 3U 10kW (40 V/250 A) power supply unit (PSU). A laptop with a MATLAB code for the PWM signal generator and opened RCbenchmark software for tracking and saving of the measurement results was connected to the system (see Figure 4.2).

Custom made metal grid was installed around the test-bench to protect people taking the measurements from unlikely event of system part detachment during the high-speed experiments. In addition, fixators for a specific EDF motor were designed and 3D-printed for accurate placement of the engine rotational axis in the middle of the test-bench for accurate measurement results.

Measurements were taken on the firmly standing table in the middle of the room, while the area in front and behind the motor was cleaned from clutter to prevent negative influence on the air flow. During the experiment an engine was power by a PWM signal with a gradually increasing duty cycle, starting from 10%. Increasing by increments of 10% the duty cycle reached all the way up to 100%, while 30 seconds has been spent between the increments to achieve more stable results.

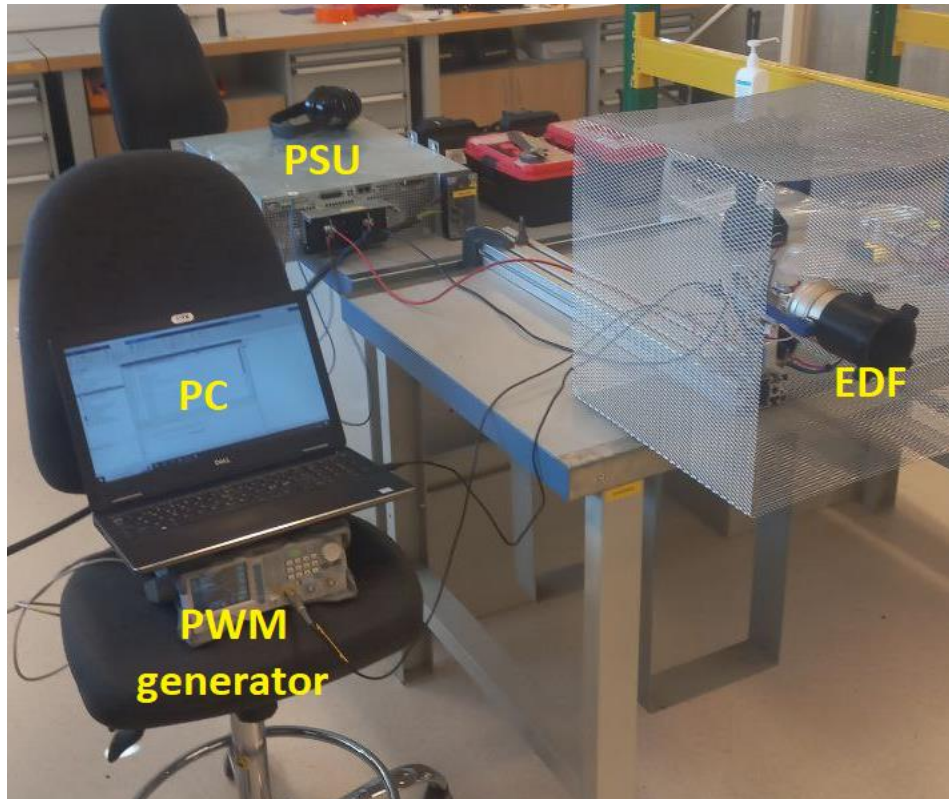


Figure 4.2 Test-bench that was used to measure thrust and torque of an EDF motor, with PSU standing for Power Supply Unit, PC for Personal Computer, EDF for Electric Ducted Fan and PWM for Pulse-Width Modulation

The data from the engine (thrust, torque, RPM) was combined with the ambient temperature measurement around the engine and a distribution board and saved as a CSV file on the computer. The data from this file has been formatted, visualized, and analyzed.

4.2 Problems and Adjustments

All main problems during an execution of the previously described experiments were related to the Electronic Speed Control (ESC) board (see Figure 4.3). ESC is one of the integral parts of an electrical motor, as it transfers constant DC power from the PSU into the 3-phase alternating voltage, required for the correct work of an electric engine. Thanks to firmware, installed on the ESC board, it also can perform some protective functions of the electric motor (e.g., overvoltage protection) and be re-programmed using external devices (e.g., programming card).

In addition to the connection to the PSU, ECS boards usually also possess a speed-control signal input. In case of the ESC in question (HobbyKing 80A (2 – 6S) ESC 4A

SBEC) that control signal type is a PWM signal, which controls the speed and thus the thrust of the brushless electrical motor in EDF. In its original installation ESC of the Dr. Mad thrust 70mm 10 blade alloy EDF, used in this work, has gotten the PWM signal from the Radio Control unit, which transmitting the signal from the remote controller. During described test PWM signal was received from the PWM generator that was controlled by a MATLAB code, as described in the Chapter 4.1. [49]

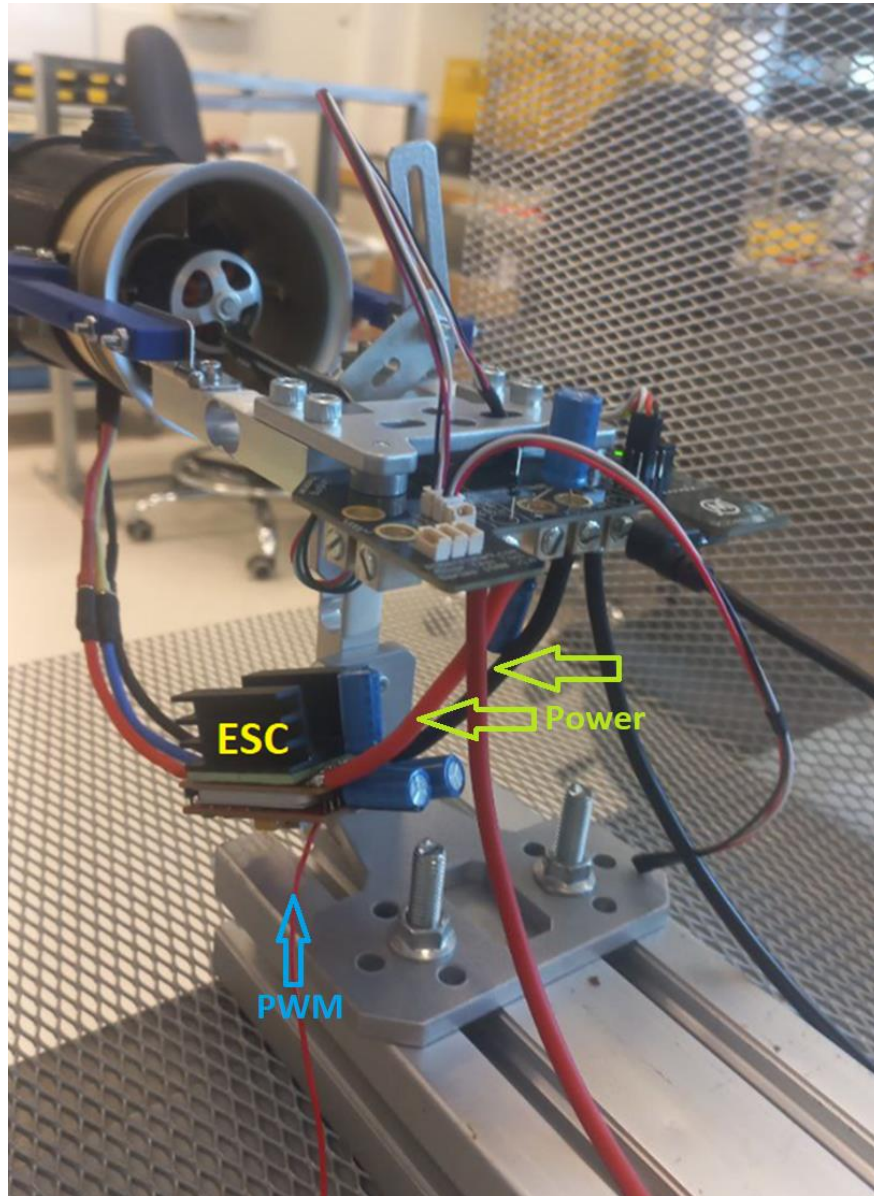


Figure 4.3 EDF motor powered through ESC board, with ESC standing for Electronic Speed Control

One of the integral parts of the ESC boards are the input capacitors. They smoothen the voltage fluctuations from the PSU unit, enabling the steady speed and robust work of an electrical engine. During the experiments capacitor legs have burned out a couple of

times due to a high impedance of the entire system and resulting high instant voltage on the individual component. Considering all of the knowledge about the capacitors following adjustments have been made to the system:

- Lead cables from the PSU to ESC have been shortened
- Diameter of the lead cables has been increased
- Capacitance of the used capacitors have been increased
- Capacitors have been soldered closer to the board (component legs has been shortened)
- Additional capacitors have been added between the PSU cables

Another problem faced during the experiment in question was also related to the ESC board functionality. As it is described in more detail in Chapter 4.4, all measured engine values (motor speed, thrust and torque) saturated between 40 and 50% duty cycle of the PWM signal. One of the plausible causes of the phenomenon is a mismatch between the maximal frequency of the PWM signal generator (25 MHz) and an ESC board. As the generator increases its frequency with increased duty cycle a plateau is achieved after it passes past the maximal frequency of the ESC board, which just cannot keep up with the pace of the generator. Such problem could be solved with a new, more powerful ESC board, which, however, is out of scope of the given work.

4.3 Results

After the ESC problems were solved, it was finally possible to perform a test run of the EDF engine. Motor optical speed, torque and thrust were measured for 11 PWM power levels starting from 0% and up-to 100% with 10% increments, while motor speed was measured in rotations per minute (RPM), torque in newton-meter (Nm) and thrust in kilogram force (kgf). Cleaned and adjusted signals can be seen on the

Figure 4.4.

On the acquired graphs the steps between 0% and 40% can be clearly seen, as the speed, thrust and torque increase with each new power level of the EDF. As discussed in Chapter 4.2, however, the ESC achieves its maximal frequency between 40% and 50%, resulting in a stagnation of all of the measurements from that point. Keeping that in mind it was decided to base all of the following calculations on the five measurements taken before the PWM duty cycle increase to 50%. In this case 40% of the PWM duty cycle would be equated to 100% of the EDF engine power, used as an input in the mathematical model. Additionally, a slight increase in power between 40% of duty cycle

and the actual peak would be excluded from the model to prevent the motor from running into the zone of relative instability of the torque, which can be seen starting around 140 seconds on the

Figure 4.4.

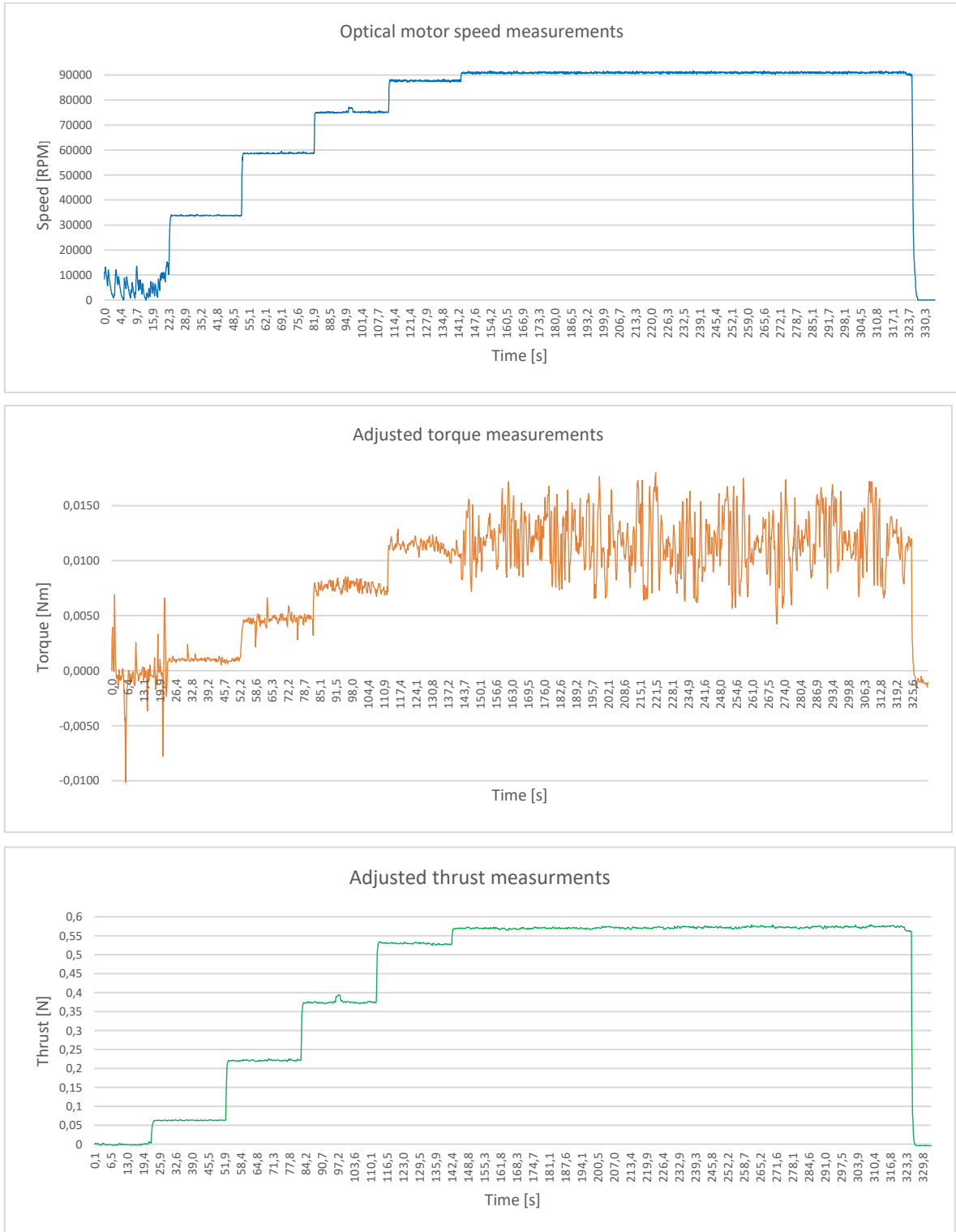


Figure 4.4 EDF motor Optical speed, Torque and Thrust measurements during an experiment

It should also be noted that in addition to rather high fluctuation of the torque by the maximal power, provided by the ESC, rather low stability was also registered at the beginning and the end of the measurements at 0% of a PWM duty cycle. This can be explained by highly unstable parasitic movements of the motor at low speeds, also seen at on the speed graph on the

Figure 4.4. For the purpose of current work those would be ignored, but some additional study could shed light on this topic. Initial assumption of the phenomenon is the problems of the wiring of the system, which became rather complicated after the introduction of three additional capacitors.

Using an average measurement value for the tracked motor indicators at different power levels Table 4-1 has been created. It should be noted that more stable values towards the end of the thirty second cycle, at which the power supplied to the motor stayed the constant, were considered. This helps to reduce the number of unwanted fluctuations in values that occur as a result of a sharp power increase. The given table also emphasizes once again the fact that values over 40% of PWM duty-cycle can be flawed (smaller increase in speed and thrust between 40% and 50%, as well as unstable torque values) and thus should be excluded from future calculations.

Table 4-1 Average motor speed, torque and thrust values for varies power levels

PWM power [%]	EDF power [%]	Motor speed [RPM]	Torque [Nm]	Thrust [kgf]
0	0	0	0	0
10	25	33750	0,0010	0,062
20	50	58650	0,0046	0,220
30	75	75000	0,0072	0,373
40	100	87500	0,0110	0,527
50	Not included	90500	Not stable	0,570

Using the value from Table 4-1 dependency graphs between the EDF power level and each of the measured values were created in Excel. For each of these graphs a polynomial trajectory lines starting from zero were generated (Equations 4.1, 4.2, 4.3), where x deals as an input (between 0 for 0% and 1 for 100% of EDF power), while quadratic equation have been chosen as a compromise between accuracy (polynomials of higher order follow the initial graph better) and ease of calculations to be performed.

Resulting physical values are expressed in the same units as the corresponding values on the

Figure 4.4 (RPM for speed, Nm for Torque and kgf for Thrust).

$$v_{motor} = -59471 \cdot x^2 + 146366 \cdot x \quad (4.1)$$

$$M_{torque} = 0,0058 \cdot x^2 + 0,0052 \cdot x \quad (4.2)$$

$$F_{thrust} = 0,2321 \cdot x^2 + 0,30343 \cdot x \quad (4.3)$$

To evaluate precision of the trajectory equations above a R-square was calculated for each of those using the build-in Excel functions. With the results between 0,9914 and 0,9994 it can be concluded that the equations in questions do in fact represent the measured values for different power levels quite precisely.

4.4 Experimental conclusions

Empirical data, acquired in the course of the experiment, represent the reality of the EDF engine functioning quite well. Although not ideal, the measured results are consistence with the expectations formed through the study of the concerned literature. Thus, keeping in mind all of the implemented simplifications, the equations 4.1, 4.2 and 4.3 are well suited for the accurate representation of the physical behavior of the tandem EDF VTOL within the constraints of the mathematical model, which is being placed in the center of the given work.

With that in mind, however, there are certain elements of the experiment that could have been done differently in order to make the process smoother and results even more dependable. Those are listed below in the form of the Lessons Learned bullets, which should be considered during upcoming electrical engine measurements in accordance with the process described in Chapter 4.1:

- Adapters that enable the motor axis arrangement right in the middle of the RCbenchmark equipment should be designed for bigger electrical motors not fitting into original equipment.
- Individual maximal frequency of the ESC should be considered during the planning of the experiment.
- Duty cycle increase of the PWM should be done in smaller intervals (e.g., 5% instead of 10%) to increase the number of reference points by the subsequent analysis.
- Shorter thicker wires should always be preferred for the connection of the PSU.

- Capacitors should be integrated into the wiring prior to testing to simplify the cabling and decrease the possibility of parasitic signals coming through.
- Shorter capacitors legs are preferred to prevent their burning through during higher voltage levels.

SUMMARY

As a result of the complexity of control mechanisms and view restrictions during the manned flights the VTOL aircraft, tail-sitters especially, have been left behind widely used classical fixed-wing and rotary-wing aircrafts. As comparably unexpensive small- and medium-sized unmanned air vehicles (UAVs) are entering a market the situation is starting to change. Due to their modest requirements towards the take-off space, compared with the fixed-wing aircraft, and superior fuel-efficiency over the rotary-wing models, VTOLs may find a much broader application in the nearest future.

Literature analysis, which can be found in the 2nd chapter of the thesis, showed a wide range of different VTOL constructions and control mechanisms, tried over the years. From the VTOL type the tail-sitter variant provides the biggest potential for smaller UAV solutions due to the smaller number of moving parts. Given work should help to tackle the main disadvantage of those VTOLs compared to tilt-wing and tilt-rotor solution – lack of robust control algorithms due to the more complicated control challenges. Usage of two counter-rotating electrical ducted fans (EDF) as a main source of power and yaw-angle control exaggerated both advantages (cheap, small, efficient) and disadvantages (harder to control) of the aircraft.

Other big outcome of the literature review was a selection of control algorithm. PID controllers, as the research show, are precise and fast enough for the given task. Simplicity of their application and a wide variety of the examples of their applications in the aircraft industry made them a perfect fit for the task of the controlling tandem EDF VTOL aircraft being in the center of this work. In addition, basic knowledge of the industry standards for the drone mathematical knowledge creation has been gathered.

In the 3rd part of the Thesis the process of model creation in MATLAB/Simulink is being discussed block-by-block, while selection of different sub-parts is being discussed in detail. The core of the model is a calculation of VTOL flight parameters using six-degrees-of-freedom equations of motion with Euler angle representation in the Airframe block. The results are then supplied to the Flying code block through Sensors applying some noise from the Environment. Flying code calculates the control signals by comparing set values with the measured signals using a system of the PID controllers. Actuators block is closing the loop by providing the signals from the PID to the EDF and servo motors, that control roll and pitch angles. Visualization block shows the described movements of the Actuators on the 3D-model representation of the tandem EDF VTOL.

Last, 4th part of the work, provides a description of the experiments, conducted in order to supply the mathematical model with the realistic physical values of the EDF engine

in question. Here, the process of measurement taking was described in detail, while problems with the Electrical Speed Controller (burning through of the capacitors and frequency differences to the PWM signal) were examined under the loop. After some iteration and adjustments, however, the results have been acquired and analyzed. EDF engine thrust, torque and speed have been increasing together with the increase of the duty-cycle of the PWM signal, as expected. Graphs of these signals were then used to describe the behavior of an engine as a function of its power input, described as a proportion of the PWM signal's duty cycle. These polynomial equations, starting from the zero, have then been successfully implemented in the mathematical model.

As the main goal of the work, developing a realistic mathematical model of the tandem EDF VTOL, has been achieved, the whole work can be said to be successful. Possibility of stable control of a VTOL with counter-rotating EDF motors on the same axis has been proven at least theoretically as a result. In addition, measurement process for the electrical engines and a visualization system for the VTOL simulation have been developed as a by-product. With that in mind, however, not all of the interesting questions could be answered in scope of these work due to the different limitations. Brief list of interesting topics requiring more detailed investigation is thus listed below:

- Introducing forward flight and transition construction features, simulations, and control algorithms for the VTOL in question.
- Tests in the wind tunnel to acquire equations to describe the behavior of the roll and pitch control surfaces more realistically.
- Tests with an ESC capable of working on higher frequencies for more accurate results of the thrust, torque, and speed measurements.
- Increasing the number of EDF engine test points would make it possible to use a map of real measurement results instead of generalized equations in the mathematical model.
- Field experiments on the real tandem EDF VTOL model could help to define if the model, developed in the course of these work, does represent the reality with good enough precision.

KOKKUVÕTE

Juhtmehhanismide keerukuse ja piiratud vaatenurga tõttu VTOL-i lennukid, eriti saba-istujad, on jäänud maha klassikalistele fikseeritud ja pöörlevate tiibadega lennukitele mehitatud lendude valdkonnas. Lennunduse demokratiseerimine viimastel aastatel on toonud turule odavaid väikse ja keskmise suurusega mehitamata õhusõidukid (UAV), mis hakkavad olukorda muutuma. Tänu nende tagasihoidlikele nõudmistele stardiruumi suhtes võrreldes fikseeritud tiibadega lennukitega ja suurema kütusesäästlikkuse tõttu võrreldes pöörlevate tiibadega mudelitega võivad VTOL-id leida lähitulevikus laiemat rakendust.

Lõputöö 2. peatükist leitav kirjandusanalüüs näitas laia valikut erinevaid VTOL-i konstruktsioone ja juhtimismehhanisme, mida on proovitud aastate jooksul. VTOL-tüüpidest pakub just saba-istuja variant oma tagasihoidliku liikuvate osade arvu tõttu suurima potentsiaali väiksemate UAV-lahenduste jaoks. Antud töö peaks aitama lahendada nende lennu masinate peamist puudust võrreldes kaldtiiva ja kaldrootori masinatega – robustse juhtimisalgoritmide puudumine keerukama juhtimise tõttu. Kahe vastassuunas pöörleva elektrilise kanaliga ventilaatori (EDF) kasutamine peamise toiteallikana ja pöördenergia juhtimiseks liialdas nii lennuki eeliseid (odav, väike, tõhus) kui ka puudusi (raskesti juhitud).

Kirjanduse ülevaate teine suur lõpptulemust oli juhtimisalgoritmi valik. PID-kontrollerid, nagu kirjandus näitab, on antud ülesande täitmiseks piisavalt täpsed ja kiired. Lisaks on PID-kontrollerite kasutamiskiirus ja levimus antud valdkonnades, mis toob endaga kaasa laia andmebaasi, teinud neid ideaalseks vahendiks selle töö keskel oleva tandem EDF mootoriga VTOL drooni juhtimiseks. Kirjanduse analüüsi käigus on lisaks ülaltoodud teadmistele kogutud ka lennunduse valdkonnas levinud droonide matemaatiliste mudelite loomise standardite põhiline arusaam.

Lõputöö 3. osas käsitletakse mudelite loomise protsessi MATLAB/Simulink platvormi kaudu. Peatükis arutletakse mudeli üldise loogilistele plokkidele põhineva struktuuri ning seletatakse konkreetsete Simulink-funktsioonide valikut. Mudeli tuumaks on drooni lennuparameetrite arvutamine, milleks on kasutusse võetud kuue vabadusastme liikumisvõrrand. See Lennukiraami plokkis asuv võrrand kalkuleerib VTOL-i täpsema positsiooni Euleri nurkade abil ning edastatakse seda Andurite plokki kaudu Lennukoodi plokki, lisades Keskkonnaplokkist tulenevat müra. Lennukood arvutab juhtimissignaale võrreldes selleks füüsiliste suuruste seatud väärtuseid sensorite kaude mõõdetud signaalidega kasutades PID-kontrollerite struktuuri. Täiturmehhanismide plokk sulgeb ahela, edastades kontrollsignaale EDF-mootoritele ja servomootoritele, mis juhivad

drooni tandem- ja rullnurka. Visualiseerimisplakk näitab täiturmeehhanismide kirjeldatud liikumisi tandem EDF VTOL 3D-mudeli peal.

Töö viimises neljandas osas kirjeldatakse katseid, mis on viidud eesmärgiga mõõta EDF mootori tegelikud füüsilised väärtused, mida eelnevalt kirjeldatud matemaatilises mudelis kasutada. Tekstis räägitakse üksikasjalikult eksperimentide protsessist, pöörates tähelepanu ka testimise käigus välju tulnud ESC probleemide peale (kondensaatorite läbipõlemine ja sageduserinevused PWM-signaaliga). Vaatamata nendele juhtudele said pärast mõningaid iteratsiooni ja kohandamisi tulemused ikkagi hangitud ja analüüsitud. EDF-i mootori tõukejõud, pöördemoment ja kiirus on ootuspäraselt kasvanud koos PWM-signaali töötsükli pikenedamisega. Lõpuks on mõõdetud signaalide graafikut kasutatud mootori käitumise kirjeldamiseks sisendvõimsusest sõltuvate funktsioonidega. Need polünoomvõrrandid on seejärel edukalt rakendatud matemaatilises mudelis Simulinki keskkonnas.

Antud lõputöö võib nimetada edukaks põhieesmärgi (tandem EDF VTOL realistliku matemaatilise mudeli väljatöötamine) saavutamise puhul. Selle tulemusena on vähemalt teoreetiliselt tõestatud samal teljel olevate vastassuunas pöörlevate EDF-mootoritega VTOL-i stabiilse juhtimise võimalikkus. Lisaks sellele on töö käigus välja töötatud elektrimootorite mõõtmisprotseduur ja drooni simulatsiooni visualiseerimiskeskond. Sellele vaatamata ei saa aga erinevate piirangute tõttu antud töö raames vastata kõigile huvitavatele küsimustele. Tulenevalt sellest on allpool toodud lühike loetelu teemadest, mis üksikasjalikumalt uurimist tulevikus nõuavad:

- Kõnealuse VTOL-i edasilennuks ja üleminekuks edasiarenemine, mis hõlmab endast konstruktsiooni, simulatsiooni ja juhtimisalgoritmi muudatusi.
- Katsed tuuletunnelis drooni käitumisele suurtematel kiirustel realistliku hinnangu andmiseks, mis võimaldab mudeli aspektide (nt. tandem- ja rullnurka kontrollpindade käitumise) täpsustamist.
- Katsed kõrgematel sagedustel töötava ESC-ga annavad täpsemaid tulemusi tõukejõu, pöördemomendi ja kiiruse mõõtmisel.
- EDF mootorite testpunktide arvu suurendamine võimaldab matemaatilises mudelis üldistatud võrrandite asemel reaalse mõõtmistulemuste kaarti kasutamist.
- Välikatsed reaalse tandem EDF VTOL mudeliga aitavad teha järeldust selle töö käigus välja töötatud mudeli täpsusest.

LIST OF REFERENCES

- [1] Federal Aviation Administration, "Aerodynamic Factors," U.S. Department of Transportation, 2012, p. 4.1-4.17. [Online]. Available: https://www.faa.gov/sites/faa.gov/files/regulations_policies/handbooks_manuals/aviation/FAA-H-8083-15B.pdf. [Accessed 28 November 2022].
- [2] Federal Aviation Administration, "Aerodynamics of Flight," U.S. Department of Transportation, 2019, p. 2.1-2.26. [Online]. Available: https://www.faa.gov/sites/faa.gov/files/regulations_policies/handbooks_manuals/aviation/helicopter_flying_handbook/helicopter_flying_handbook.pdf. [Accessed 28 November 2022].
- [3] Z. Yaoming, Z. Haoran and L. Yaolong, "An evaluative review of the VTOL technologies for unmanned and manned aerial vehicles," *Computer Communications*, vol 149, pp. 356-369, January 2020.
- [4] G. J. J. Ducard and M. Allenspach, "Review of designs and flight control techniques of hybrid and convertible VTOL UAVs," *Aerospace Science and Technology*, vol 118, p. 107035, November 2021.
- [5] R. F. Dorr, "DefenceMediaNetwork," 8 November 2016. [Online]. Available: <https://www.defensemmedianetwork.com/stories/tail-sitter-xfy-1-pogo-xfv-1/>. [Accessed 1 Detseember 2022].
- [6] W. Wang, J. Zhu and M. Kuang, "Design, modelling and hovering control of a tail-sitter with single thrust-vectorred propeller," in *International Conference on Intelligent Robots and Systems*, Vancouver, 2017.
- [7] W. E. Green and P. Y. Oh, "MAV That Flies Like an Airplane and Hovers Like a Helicopter," in *International Conference on Advanced Intelligent Mechatronics*, Monterey, 2005.
- [8] H. Liu, F. Peng, F. L. Lewis and Y. Wan, "Robust Tracking Control for Tail-Sitters in Flight Mode Transitions," *Transactions on Aerospace and Electronic Systems*, vol. 55, no. 4, pp. 2023-2035, 2019.

- [9] A. Manouchehri, H. Hajkarami and M. S. Ahmadi, "Hovering control of a ducted fan VTOL Unmanned Aerial Vehicle (UAV) based on PID control," in *International Conference on Electrical and Control Engineering*, Yichang, 2011.
- [10] R. Naldi, L. Gentili, L. Marconi and A. Sala, "Design and experimental validation of a nonlinear control law for a ducted-fan miniature aerial vehicle," *Control Engineering Practice*, vol. 18, pp. 747-760, 2010.
- [11] S. Verling, T. Stastny, G. Bättig, K. Alexis and R. Siegwart, "Model-based transition optimization for a VTOL tailsitter," in *International Conference on Robotics and Automation*, Singapore, 2017.
- [12] J. Liang, Q. Fei, B. Wang and Q. Geng, "Tailsitter VTOL Flying Wing Aircraft Attitude," in *Youth Academic Annual Conference of Chinese Association of Automation*, Wuhan, 2016.
- [13] L. Ximin, G. Haowei, W. Ya, L. Zexiang, S. Shaojie and Z. Fu, "Design and Implementation of a Quadrotor Tail-sitter VTOL UAV," in *International Conference on Robotics and Automation*, Singapore, 2017.
- [14] Z. Li, W. Zhou, H. Liu, L. Zhang and Z. Zuo, "Nonlinear Robust Flight Mode Transition," *IEEE Access Vol.6*, vol. 6, pp. 65909 - 65921, 2018.
- [15] W. Xu, H. Gu, Y. Qing, J. Lin and F. Zhang, "Full Attitude Control of an Efficient Quadrotor Tail-sitter VTOL UAV," in *International Conference on Unmanned Aircraft Systems*, Atlante, 2019.
- [16] Y. Song and H. Wang, "Design of Flight Control System for a Small Unmanned Tilt Rotor Aircraft," *Chinese Journal of Aeronautics*, vol. 22, pp. 250-256, 25 March 2009.
- [17] T. Nerep, "Construction of VTOL Drone With Tandem EDF Motor and Development of an Algorithm for Automatic Stabilization in Hover Flight," Tallinn University of Technology, Tallinn, 2022.
- [18] G. Flores, I. Lugo and R. Lozano, "6-DOF Hovering Controller Design of the Quad Tiltrotor Aircraft:," in *Conference on Decision and Control*, Los Angeles, 2014.
- [19] C. Chao, S. Lincheng, Z. Daibing and Z. Jiyang, "Mathematical Modeling and Control of a Tiltrotor UAV," in *International Conference on Information and Automation*, Ningbo, 2016.

- [20] A. S. Onen, L. Cevher, M. Senipek, T. Mutlu, O. Gungor, I. O. Uzunlar, D. F. Kurtulus and O. Tekinalp, "Modeling and Controller Design of a VTOL UAV," in *International Conference on Unmanned Aircraft Systems*, Denver, 2015.
- [21] K. Muraoka, N. Okada and D. Kubo, "Quad Tilt Wing VTOL UAV: Aerodynamic Characteristics," in *Infotech@Aerospace Conference*, Seattle, 2009.
- [22] D. Rohr, T. Stastny, S. Verling and S. Roland, "Attitude and Cruise Control of a VTOL Tiltwing UAV," *IEEE Robotics and Automation Letters*, vol. 4, no. 3, pp. 2683-2690, 2019.
- [23] C. Xiang, W. Fan, H. Liu, B. Xu and N. Huang, "Modeling and Simulation Analysis of an Unmanned Tandem Ducted," in *International Conference on Unmanned Aircraft Systems*, Denver, 2015.
- [24] B. Xu, X. Wang, C. Xiang, Y. Ma and W. Chen, "Modelling and Hovering Control of a Novel Multi-Tandem Ducted," in *International Conference on Unmanned Aircraft Systems*, Denver, 2015.
- [25] Y. Zhang, C. Xiang, B. Xu, X. Wang and W. Fan, "Comprehensive Nonlinear Modeling and Attitude Control of a Novel," in *International Conference on Aircraft Utility Systems*, Beijing, 2016.
- [26] A. Jain, K. Bavikar, A. Sanjay, M. Gupta, B. R. Gupta and H. Dineshkumar, "Baseline procedure for conceptual designing of an eVTOL for Urban Air Mobility," in *International conference of Electronics, Communication and Aerospace Technology*, Coimbatore, 2020.
- [27] M. Lihulinn, "Construction of Tandem EDF engine," Estonian Aviation Academy, Tartu, 2018.
- [28] J. T. Khan, "Electrical and Mechanical Design of Multipurpose Ducted-Fan Type VTOL UAV," in *Canadian Conference on Electrical and Computer Engineering*, Niagara Falls, 2011.
- [29] A. Bonci, A. Cervellieri, S. Longhi, G. Nabissi and G. A. Scala, "The Double Propeller Ducted-Fan, an UAV for safe Infrastructure inspection and human-interaction," in *International Conference on Emerging Technologies and Factory Automation*, Vienna, 2020.

- [30] S. W. Sung, J. Lee and I.-B. Lee, *Process Identification and PID Control*, Singapore: Wiley-IEEE Press, 2009.
- [31] Z. Cheng, H. Pei and S. Li, "Neural-Networks Control for Hover to High-Speed-Level-Flight Transition of Ducted Fan UAV With Provable Stability," *IEEE Access*, vol. 8, pp. 100135 - 100151, 2020.
- [32] J. M. O. Barth, J.-P. Condomines, M. Bronz, L. R. Lustosa, J.-M. Moschetta, C. Join and M. Fliess, "Fixed-wing UAV with transitioning flight capabilities : Model-Based or Model-Free Control approach? A preliminary study," in *International Conference on Unmanned Aircraft Systems* , Dallas, 2018.
- [33] Y. Ke, K. Wang, K. Gong, S. Lai and B. M. Chen, "Model Based Robust Forward Transition Control for Tail-Sitter Hybrid Unmanned Aerial Vehicles," in *International Conference on Control & Automation*, Ohrid, 2017.
- [34] A. Oosedo, S. Abiko, A. Konno, T. Koizumi, T. Furui and M. Uchiyama, "Development of a quad rotor tail-sitter VTOL UAV without control surfaces and experimental verification," in *International Conference on Robotics and Automation*, Karlsruhe, 2013.
- [35] S. Zhang, Q. Fei, J. Liang and Q. Geng, "Modeling and control for longitudinal attitude of a twin-rotor tail-sitter unmanned aerial vehicle," in *International Conference on Control & Automation*, Ohrid, 2017.
- [36] IBM Cloud Education, "IBM," 17 August 2020. [Online]. Available: <https://www.ibm.com/cloud/learn/neural-networks>. [Accessed 02 Detseember 2022].
- [37] J. Xu, T. Du, M. Foshey, B. Li, B. Zhu, A. Schulz and W. Matusik, "Learning to Fly: Computational Controller Design for Hybrid UAVs with Reinforcement Learning," *ACM Trans. Graph.*, vol. 38, pp. 1-12, 2019.
- [38] R. Gordon and M. Carone, "Quadcopter Simulation and Control Made Easy - MATLAB and Simulink Video," 1 May 2017. [Online]. Available: https://www.youtube.com/watch?v=fpJZSQmqDvk&ab_channel=MATLAB. [Accessed 25 February 2023].
- [39] B. Douglas, "Drone Simulation and Control, Part 5: Tuning the PID controller," 20 November 2018. [Online]. Available: <https://www.youtube.com/watch?v=BqrRfoH->

19s&list=PLPNM6NzYyzYqMYNc5e4_xip-
yEu1jiVrr&index=5&ab_channel=MATLAB. [Accessed 25 February 2023].

- [40] MathWorks, "MathWorks Help Center," [Online]. Available: <https://se.mathworks.com/help/aeroblks/6dofeulerangles.html>. [Accessed 15 April 2023].
- [41] A. Tousif, A. Md. Tanjin, I. S.M. Rafiul and A. Shabbir, "Computational Study of Flow Around a NACA 0012 Wing Flapped at Different Flap Angles with Varying Mach Numbers," *Global Journal of Researches in Engineering*, vol. IV, no. 13, pp. 5-15, 2013.
- [42] C. Rumsey, "2DN00: 2D NACA 0012 Airfoil Validation Case," 8 September 2022. [Online]. Available: https://turbmodels.larc.nasa.gov/naca0012_val.html. [Accessed 15 April 2023].
- [43] A. A. de Paula, „The airfoil thickness effects on wavy leading edge phenomena at low Reynolds,“ University of São Paulo, São Paulo, 2016.
- [44] MathWorks, "MathWorks Help Center," [Online]. Available: <https://se.mathworks.com/help/aeroblks/wgs84gravitymodel.html>. [Accessed 16 April 2023].
- [45] MathWorks, "MathWorks Help Center," [Online]. Available: <https://se.mathworks.com/help/aeroblks/windshearmodel.html>. [Accessed 17 April 2023].
- [46] D. Briassoulis, A. Mistriotis and A. Giannoulis, "Wind forces on porous elevated panels," *Journal of Wind Engineering and Industrial Aerodynamics*, no. 98, pp. 919-928, 2010.
- [47] MathWorks, "MathWorks Help Center," [Online]. Available: <https://se.mathworks.com/help/simulink/slref/bandlimitedwhitenoise.html>. [Accessed 18 April 2023].
- [48] Tyto Robotics , "Series 1580 Test Stand Datasheet," 09 May 2022. [Online]. Available: [https://cdn.rcbenchmark.com/landing_pages/Manuals/Series%201580%20Data sheet.pdf](https://cdn.rcbenchmark.com/landing_pages/Manuals/Series%201580%20Data%20sheet.pdf). [Accessed 09 April 2023].

- [49] HobbyKing.com, "HobbyKing.com," [Online]. Available: https://hobbyking.com/en_us/hobbyking-80a-2-6s-esc-4a-sbec.html. [Accessed 23 April 2023].
- [50] Z. Liu, D. Theilliol, L. Yang, Y. He and J. Han, "Transition Control of Tilt Rotor Unmanned Aerial Vehicle Based on Multi-Model Adaptive Method," in *International Conference on Unmanned Aircraft Systems*, Miami, 2017.

APPENDICES

Appendix 1 Technical drawing of the Affixer for the EDF motor

